CHARLES UNIVERSITY
Faculty of Pharmacy in Hradec Králové
Department of Organic and Bioorganic Chemistry

Diploma Thesis

Quantification of Skin Lipids in Mouse Model of Induced Psoriasis

Mohammadreza Shojaei

Supervisor: PharmDr. Lukáš Opálka, Ph.D
Consultant: PharmDr. Pavla Jančálková
Hradec Králové 2024

I hereby declare that this thesis is my original work which I solely composed by myself under the supervision of PharmDr. Lukáš Opálka, Ph.D.
All used literature and other sources are summarized in the list of references and properly cited.
This work has not been submitted for any different or equal degree.

Hradec Králové Mohammadreza Shojaei

ACKNOWLEDGMENTS

I would like to express my sincere gratitude to my supervisor, PharmDr. Lukáš Opálka, Ph.D., for his professional guidance, invaluable advice, patience, willingness, and helpfulness throughout the development of this thesis.

Additionally, I would like to extend my heartfelt thanks to my family. Their unwavering support has been a pillar of strength for me throughout this journey. My wife, in particular, has been a constant source of encouragement and love, providing me with the motivation to persevere through challenging times. Her belief in my abilities has been invaluable.

I am also deeply grateful to my parents, whose sacrifices and dedication have laid the foundation for my educational pursuits. Their continuous support and encouragement have been instrumental in my achievements.

A special thanks to my in-laws for their guidance and insightful advice. Their wisdom and experience have been a significant influence, and their support has been greatly appreciated.

ABSTRACT

Charles University, Faculty of Pharmacy in Hradec Králové	
Department of	Organic and Bioorganic Chemistry
Candidate	Mohammadreza Shojaei
Supervisor	PharmDr. Lukáš Opálka, Ph.D.
Advisor	PharmDr. Pavla Jančálková
Title of Diploma Thesis	Quantification of skin lipids in mouse model of induced psoriasis

Ceramides are essential lipid components in the stratum corneum of human skin, playing a critical role in maintaining the skin's barrier function. Alterations in the absolute levels and the ratio of various ceramide subclasses have been linked to the disruption of this barrier, contributing to the pathogenesis of psoriasis. This study primarily aimed to investigate the therapeutic potential of exogenous Acylceramide EOS, delivered via a topical cream, in mouse models with induced psoriasis. Furthermore, the research sought to compare the ceramide profiles in the stratum corneum between healthy mice and those with induced psoriasis.

Specific objectives included quantifying selected ceramide subclasses and analyzing them based on acyl chain length, sphingoid base content, degree of hydroxylation, and the ratio of changes between long-chain and ultra-long-chain ceramides. The study involved 12 mice, divided into four groups of three, each receiving different treatments: the first group served as the control with no treatment, the second group received only Imiquimod to induce psoriasis, the third group received Imiquimod along with a blank cream, and the fourth group was treated with Imiquimod and ceramide EOS29 cream.

Strip tapes were collected from a consistent location on the dorsal side of each mouse for protein content determination. Ceramides were then extracted using a mixture of organic solvents and analyzed through LC-MS/MS with the inclusion of internal standards. This analysis focused on quantifying specific ceramide subclasses and evaluating them concerning the average acyl chain length, individual sphingoid base content, and degree of hydroxylation.

Our results indicate a potential involvement of phytosphingosine ceramides in the skin barrier dysfunction of the mouse stratum corneum with induced psoriasis. Although the application of 0.5% ceramide EOS cream did not result in an improvement in transepidermal water loss, it did alter the ceramide profile compared to other treatment groups and improved the ratio of long-chain to ultra-long-chain ceramides.

ABSTRAKT

Univerzita Karlova, Farmaceutická fakulta v Hradci Králové.	
Katedra	organické a bioorganické chemie
Kandidát	Mohammadreza Shojaei
Vedoucí práce	PharmDr. Lukáš Opálka, Ph.D.
Konzultant	PharmDr. Pavla Jančálková
Název diplomové práce	Kvantifikace kožních lipidů v myším modelu indukované psoriázy

Ceramidy jsou základními lipidy ve stratum corneum lidské kůže, které hrají klíčovou roli v udržování bariérové funkce kůže. Změny v absolutních hladinách a poměru různých podtříd ceramidů jsou spojovány s narušením této bariéry, což přispívá k patogenezi psoriázy. Tato studie se primárně zaměřila na zkoumání terapeutického potenciálu exogenního acylceramidu EOS, aplikovaného topicky prostřednictvím krému u myších modelů s indukovanou psoriázou. Dále se výzkum snažil porovnat profily ceramidů stratum corneum mezi zdravými myšmi a těmi s indukovanou psoriázou.

Konkrétní cíle zahrnovaly kvantifikaci vybraných podtříd ceramidů a jejich analýzu na základě délky acylového řetězce, typu sfingoidní báze, stupně hydroxylace a poměru změn mezi dlouhými a ultra-dlouhými ceramidy. Studie zahrnovala 12 myší, rozdělených do čtyř skupin po třech, přičemž každá skupina obdržela odlišnou léčbu: první skupina sloužila jako kontrolní bez léčby, druhá skupina dostala pouze Imiquimod k indukci psoriázy, třetí skupina dostala Imiquimod spolu s krémem bez účinné látky a čtvrtá skupina byla léčena Imiquimodem a krémem s EOS29.

Vzorky z náplastí byly odebrány ze stejného místa na hřbetní straně každé myši pro stanovení obsahu proteinů. Ceramidy byly následně extrahovány pomocí směsi organických rozpouštědel a analyzovány metodou LC-MS/MS za použití vnitřních standardů. Tato analýza se zaměřila na kvantifikaci specifických podtříd ceramidů a jejich hodnocení vzhledem k průměrné délce acylového řetězce, obsahu jednotlivých sfingoidních bází a stupni hydroxylace.

Naše výsledky naznačují možnou účast fytosfingozinových ceramidů v dysfunkci kožní bariéry ve stratum corneum myší s indukovanou psoriázou. Ačkoli aplikace krému s 0,5% ceramide EOS nevedla ke zlepšení transepidermální ztráty vody, změnila ceramidový profil lipidů ve srovnání s ostatními skupinami myší a zlepšila poměr dlouhých ceramidů k ultra-dlouhým ceramidům.

Table of Contents

LIST OF ABBREVIATIONS

AD	Atopic dermatitis
CD	Corneodesmosome
CE	Cornified envelope
CER	Ceramide
CerS	Ceramide synthase
CHOL	Cholesterol
CLE	Corneocyte lipid envelope
DEGS	Dihydroceramide desaturase
ELOVL	Very long chain Fatty acid Elongase
FFA	Free fatty acid
FLG	Filaggrin
GlcCER	Glucosylceramide
HPLC	High-performance liquid chromatography
HPTLC	High-performance thin-layer chromatography
KAR	3-ketoacyl-CoA reductase
KDS	3-ketodihydrosphingosine
KDSR	3-ketodihydrosphingosine Reductase
LBs	Lamellar bodies
LC/MS	Liquid chromatography-mass spectrometry
LC/MS/MS	Liquid chromatography with tandem mass spectrometry
LCB	Long-chain base
LOX	Lipoxygenase
NMF	Natural moisturizing factor
PNPLA1	Patatin-like phospholipase domain-containing protein 1
PSO	Psoriasis
S1P	Sphingosine-1-phosphate
SB	Stratum Basale
SC	Stratum Corneum
SG	Stratum Granulosum
SL	Stratum Lucidum
SM	Sphingomyelin
Sph	Sphingosine
SPT	Serine-palmitoyl transferase
SS	Stratum spinosum
TEWL	Transepidermal water Loss
ULCFA	Ultra-long chain fatty acid
VLCFA	Very long chain fatty acid

1. INTRODUCTION AND OBJECTIVE OF THE WORK

The skin, the largest organ of the human body, serves as a crucial barrier against the external environment and maintains internal homeostasis. The stratum corneum (SC), the outermost layer, is primarily responsible for this barrier function. Compromised barrier function, due to alterations in lipid composition and organization, is indicative of various skin disorders, including psoriasis, which is characterized by abnormal epidermal differentiation, hyperproliferation, vasodilation, and inflammatory cell infiltration, and it has been associated with metabolic syndrome, obesity, insulin resistance, and cardiovascular diseases, potentially increasing mortality risk in severe cases.[1]

Altered sphingolipid levels have been observed in psoriasis patients, suggesting that quantifying skin lipids could provide crucial insights into psoriasis pathogenesis and potential treatments. Topical applications of ceramides and pseudoceramides, which are structurally similar, have been used to treat conditions such as xerosis, psoriasis, and atopic dermatitis. These compounds enhance skin barrier function by forming liquid crystalline structures, lamellar liquid crystalline structures, and gel structures, thereby creating an effective permeability barrier. Ceramides can localize on the skin surface, integrate into SC multilamellar structures, and penetrate the stratum granulosum, becoming precursors to endogenous ceramide synthesis. The absorption of exogenous ceramides depends on skin barrier integrity and product formulation, where they are metabolized into sphingoid bases and fatty acids for endogenous ceramide synthesis. Therefore, selecting appropriate ceramide molecular species is crucial for the formulation of effective topical treatments.[2-4]

The primary objective of this study is to evaluate the effect of exogenous Acylceramide EOS, applied via topical cream, on mouse model with induced psoriasis. Additionally, the study aimed to compare the ceramide profile in the stratum corneum of healthy mice to that of mice with induced psoriasis. Specific goals included quantifying selected ceramide subclasses and analyzing them in terms of acyl chain length, sphingoid base content, degree of hydroxylation, and changes in the ratio of long-chain to ultra-long-chain ceramides.

2. THE CURRENT STATE OF KNOWLEDGE

2.1 Skin

The skin, being the body's largest organ, spans its entire external surface. It consists of three layers: the epidermis, the dermis, and the hypodermis. Each layer has distinct anatomical and functional properties. The complex structure of skin forms a versatile barrier with two main functions: firstly, against outside threats such as ultraviolet (UV) radiation, microbes, allergens, and xenobiotics as well as physical trauma. Secondly, maintaining homeostasis inside of the body including thermoregulation, and prevention of excessive water loss through the skin known as transepidermal water loss (TEWL).[5,6]

The hypodermis lies beneath the dermis as the deepest layer of the skin. This layer incorporates adipose lobules and houses certain skin appendages such as hair follicles, sensory neurons, and blood vessels.[5] The hypodermis primarily serves to protect against mechanical injury and provide thermal insulation. Additionally, it offers support and supplies energy for the body via stored fat cells.[7]

The dermis, being the middle layer, is primarily divided into two layers: the papillary layer and the reticular layer. The papillary dermis is in contact with the epidermis and is primarily composed of loose connective tissue and blood vessels. In contrast, the reticular layer which is situated deeper forms a thick layer of dense connective tissue with collagen fibers, making up the majority of the dermis.[8] These layers together act as foundational support for the epidermis, linking it to the underlying hypodermis. Within the dermis reside sweat glands, hair follicles, muscles, sensory neurons, and blood vessels. Through its vascular network, the dermis supplies vital nutrients to the epidermis and facilitates ongoing intercellular communication between the two layers.[5,9]

The epidermis is a stratified and squamous multi-layered epithelium that harbors various types of cell populations including Keratinocytes which constitute the majority of cells in the epidermis, as well as Melanocytes, Langerhans' cells, and Merkel's cells.[10] Keratinocytes are polygonal in shape with large, round nuclei. They are connected by protein structures called desmosomes, which help them adhere more tightly to one another.[7]

Moreover, derived from the morphology and position of keratinocytes during the differentiation process, the classification of 4 layers based on depth can be outlined, extending from the deepest to the superficial portion of the epidermis, namely stratum basale (SB), stratum spinosum (SS), stratum granulosum (SG), and stratum corneum (SC).[10] Additionally,

beyond the typical four primary layers of the epidermis, the stratum lucidum (SL) layer may also be present, predominantly found in the thick epidermal layer of certain anatomical regions such as the palm and sole.[5] The basal layer serves as the main site of mitotically active cells in the epidermis, generating cells for the outer epidermal layers. Initially, proliferating Keratinocytes in their most rudimentary form are situated within the basal layer and subsequently, undergo sequential differentiation as they progress toward the stratum corneum.[10] Eventually, cornification takes place and anucleated corneocytes are formed which are terminally differentiated keratinocytes, and technically considered dead cells.[11] Consequently, the SB, SS, and SG constitute the viable epidermis whereas the SL and SC are classified as the non-viable epidermis, with SC representing the endpoint of differentiation.[1]

2.2 Stratum Corneum

The human SC is comprised of layers of corneocytes embedded within a matrix of lipid-enriched lamellar sheets.[13] (**Figure 1**) The structure of the SC is often referred to as a "bricks and mortar" arrangement, where the lipids represent the mortar and corneocytes are the bricks.[14]

Corneocytes are interconnected by corneodesmosomes (CDs) and are characterized by their flattened shape, filled with keratin filaments. These corneocytes are encased in a peripheral protein envelope called the cornified envelope (CE). It was previously believed that the CE was further esterified to a monolayer of lipids known as the corneocyte lipid envelope (CLE) via transesterification.[15,16] In a recent study by Takeichi et al., the authors concluded that the enzyme SDR9C7 is essential for skin barrier formation by catalyzing the NAD^+-dependent dehydrogenation of Acylceramides. This critical step involves a Michael addition, facilitating the production of a specific Acylceramide containing an epoxy-enone necessary for non-enzymatic coupling to proteins. Mutations in SDR9C7, as observed in ichthyosis patients and Sdr9c7 knockout mice, result in the loss of covalent binding of epidermal ceramides to proteins, leading to structural defects in the skin barrier. These findings provide significant insights into the mechanisms of skin barrier formation and the pathogenesis of related skin diseases.[17]

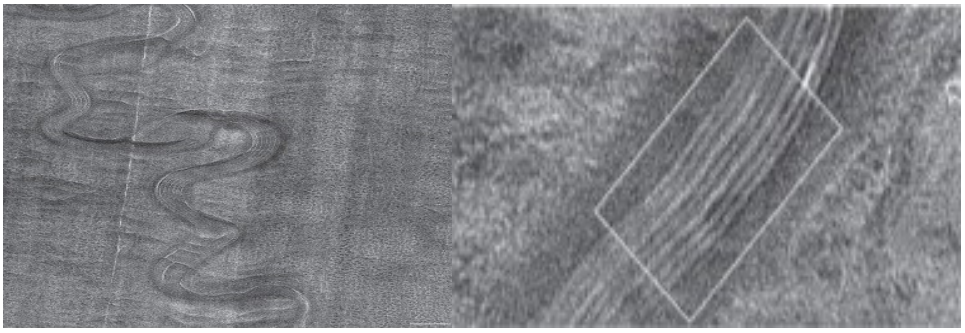

Figure 1.Cryo-electron microscopy of vitreous skin sections (CEMOVIS) reveals the intensity pattern of the stratum corneum's extracellular lipid matrix, consisting of folded, stacked layers called lamellar sheets. On the left: Medium-magnification CEMOVIS micrograph showing the interface between two corneocytes in the stratum corneum. On the right: High-magnification CEMOVIS micrograph of the extracellular space in the stratum corneum. Adapted from the Journal of Investigative Dermatology.[18]

Cornification is a specific programmed cell death of keratinocytes, which takes place through three primary events. Initially, within the keratinocyte, a network comprised of keratin filaments is formed, which is accompanied by the loss of organelles. At the same time, the premature CE, which was formed beneath the keratinocyte's plasma membrane, through the covalent attachment of specific precursor proteins, matures into a rigid structure and replaces the cell membrane.[13] Formation and selective degradation of CDs is the final event in the process of cornification.[15,19]

The SC, being the body's primary defense mechanism, is a critical barrier against the external environment.[11] Together, Corneocytes and CDs provide the mechanical resistance of the layer, while intercellular lipids are accountable for the skin's barrier function. The lipid matrix within the SC represents the only continuous pathway for the penetration of externally applied chemicals to the skin.[15] It's important to note that in healthy individuals, TEWL from the SC is effectively regulated by this barrier.[16] As a result, disruption of this barrier can lead to dehydration, inflammation, and skin diseases such as atopic dermatitis (AD) and psoriasis (PSO).[20]

Resilience and firmness of the SC are ensured due to the presence of CE,[15] which is composed of densely interconnected proteins like filaggrin (FLG), involucrin (IVL), loricrin (LOR), and small proline-riched protein (SPR).[21] FLG has a critical role in the alignment of keratin filaments. Alternatively, its metabolites are part of the natural moisturizing factor (NMF), which is crucial for maintaining optimal hydration levels within the SC.[13] Several clinical studies and research findings have shown that FLG deficiency correlated with impaired composition and organization of SC lipids, resulting in decreased levels of NMF, increased skin surface pH, and reduced skin hydration.[22] The CE, on the interior surface, is intertwined with the bundles of keratin filaments,[16] while on the exterior surface, is covalently attached to

CLE, which consists of protein-bound ω-hydroxyceramides.[23] These protein-bound lipids, potentially serve as a framework for the intercellular lipid lamellae.[24]

The lipid composition of the extracellular matrix in the SC, with its notably scarce levels of phospholipids, is distinct and significantly differs from that of most biological membranes.[25] The lipid matrix primarily consists of three lipid classes known as ceramides (CERs), cholesterol (CHOL), and free fatty acids (FFAs) found in an approximately equimolar ratio. These lipids constitute 45-50%, 25%, and 10-15% by weight, respectively. Additionally, a small amount of other lipids are present, with CHOL esters and CHOL sulfate being the most significant.[16,26] The lipid composition of SC is pivotal for maintaining epidermal homeostasis, as deviations from this equilibrium have resulted in compromised barrier function in various skin diseases, such as PSO, AD, and several types of ichthyosis.[27,28] Compared to membranes enriched with phospholipids, the SC has prominently lower fluidity and permeability, which is attributed to its distinct lipid composition, in particular its abundance of lipids with saturated very long chains, such as CERs. However, CHOL can provide essential fluidity to the layer, which might otherwise be excessively rigid and potentially brittle.[16]

Skin lipids are synthesized within the keratinocytes in the SS. They are initially converted into more polar precursors in the SG and later revert to a non-polar mixture in the extracellular space of the SC.[21,29] At the border between SS/SG, lamellar bodies (LBs) begin to form,[7] initially appearing in the SS, and increasing in number as differentiation progresses into the SG. These ovoid granules, found exclusively in the epidermis,[28] consist of a bounding membrane unit and contain layers of lamellar lipid disks alongside several hydrolytic enzymes. At the boundary between SG/SC, the contents of the LBs are extruded into the intercellular space of SC.[23] (**Figure 2**) Their content includes phosphoglycerides, sphingomyelins, glucosylceramides, and free sterols, as well as acid hydrolases like β-glucocerebrosidase, sphingomyelinase, and phospholipase A_2, along with proteases and antimicrobial peptides such as defensin.[26,30] Here, with the help of specific mediators like co-secreted catabolic enzymes, lipid precursors are converted into non-polar lipid products, forming an extracellular multilamellar lipid matrix.[26] Notably, β -glucocerebrosidase converts glucosylceramides into ceramides, acidic sphingomyelinase likewise transforms sphingomyelin into ceramides, and phospholipase breaks down phospholipids into FFAs and glycerol.[16,25] Following the release of LB's content, there is a complex change in the lipid composition, leading to the formation of patterned lamellar sheets from short membrane stacks.[16] These lipids assemble into a structured framework parallel to corneocytes known as lipid lamellae,[31] characterized by lateral

and lamellar lipid organization. The arrangement of these lipids within the lipid lamellae is influenced by their composition.[24]

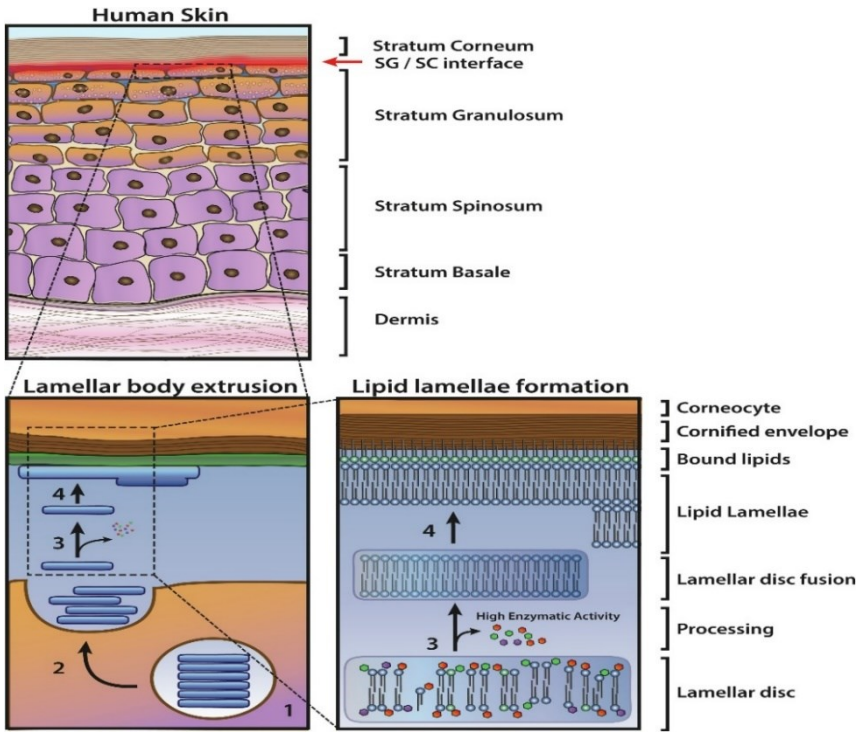

Figure 2. Schematic representation of the epidermal cross-section, including the lamellar body extrusion process and subsequent lipid lamellae formation. This figure highlights the cellular mechanisms involved in the production and organization of lipid layers within the stratum corneum. Adapted from Progress in Lipid Research journal.[3]

Phospholipid breakdown yields glycerol and FFAs, with the latter contributing to the acidic nature of the SC which is typically around pH 4-5.5.[13] This acidic environment is crucial for enzyme regulation. For instance, the highest activity of enzymes like β-glucocerebrosidase and acidic sphingomyelinase occurs at a pH of 5.1-5.6,[29] therefore, any increase in the SC pH reduces the activity of these enzymes, altering the extracellular processing of lipids and compromising barrier function.[25]

FFAs also known as non-esterified fatty acids (NSFAs) in the human SC, consist of single carbon chains predominantly saturated and unbranched varying in length from approximately 16 to 36 carbon atoms.[32] The most prevalent chain lengths are 24C and 26C, lignoceric acid, and cerotic acid, respectively.[26] The distinctive composition of FFAs in SC sets it apart from those found in serum or sebum, suggesting that these fatty acids are synthesized *de novo* within the epidermis.[29] Alongside saturated FFAs, which constitute the majority, hydroxy-FFAs, monounsaturated fatty acids (MUFAs), and minimal quantities of polyunsaturated fatty acids (PUFAs) such as linoleic acid are present. Hydroxy-FFAs and MUFAs collectively account for no more than 25% of the total FFA content.[24]

CHOL is the second major lipid class and the primary sterol in the SC. While it can be acquired from nutritional sources, epidermal CHOL is predominantly synthesized within the epidermis.[29] Both high and low levels of CHOL can disrupt barrier function.[26] Initially sulfated in the lower epidermis, CHOL is converted back to its original form through desulfation in the outer epidermis.[33] Although the amount of CHOL sulfate in the epidermis is relatively low, it is crucial for the cell-cell cohesion of the SC.[29] Disruption of this "cholesterol sulfate cycle" leads to both permeability barrier abnormalities,[33] as well as abnormal desquamation which underscores the crucial role of the CHOL sulfate in the desquamation regulation.[25]

2.3 Ceramides

CERs are vital constituents of the eukaryotic cell membrane and are present in all mammalian tissues. While they constitute a small portion in most tissues, their diversity is prominent in the epidermis,[28,34] and their most abundant localization is in the SC.[35,36] CER levels notably rise during keratinocyte differentiation.[28]

2.3.1 Function

As mentioned previously, the epidermal barrier serves multiple purposes and CERs' significance lies in their pivotal role in maintaining the homeostasis of this barrier, including forming the CLE and multilamellar sheets. In addition to their critical function in forming and preserving skin barrier integrity, CERs, and their derivatives such as S1P (Sphingosine-1-phosphate), which is derived from the hydrolysis of CERs, are implicated in cellular signaling processes and are associated with cell proliferation, differentiation, and apoptosis in the human epidermis. There's a clear distinction between CERs functioning in the multilamellar barrier outside cells and those acting as second messengers inside cells.[20,37]

2.3.2 Structure

CERs, the central component in sphingolipid metabolism,[38] are a structurally diverse and complex group of sphingolipids comprised of an acyl chain (FA) connected through an amide bond to a sphingoid base, also known as a long-chain base (LCB).[39] The head groups of ceramides are small and include multiple functional groups capable of forming lateral hydrogen bonds with nearby ceramide molecules.[40] Currently, in humans, more than 20 CER subclasses have been identified and classified based on their specific combinations of LCBs and FAs.[26] (**Figure 3**) Their heterogeneity arises from differences in chain lengths, degree of unsaturation,

and the position and number of hydroxyl groups of both the FA and the LCB,[16,28,29] resulting in the identification of more than a thousand CER species.[41,42]

In mammals, 5 types of LCBs have been identified. These sphingoid bases are long-chain amino alcohols characterized by two hydroxyl groups at the C1 and C3 positions and an amino group at the C2 position. This structural pattern which serves as the basis for other LCBs, represents dihydrosphingosine (dS), also referred to as sphinganine. Alongside dS, significant LCBs in the SC include Sphingosine (S), marked by a trans double bond between the C4 and C5 positions, Phytosphingosine (P) with an additional hydroxyl group at the C4 position, 6-Hydroxy sphingosine (H), which features both a trans double bond between the C4 and C5 positions and an extra hydroxyl group at C6, and the later discovered 4,14-sphingadiene (SD), containing two double bonds positioned at C4 and C14.[34,41,47] However, it's worth noting that SD was detected at very low levels in the SC.[43]

Regarding their localization, S, being the major LCB in mammals, and dS, present at lower levels, are ubiquitous in human tissues, P, in addition to the skin, is widely distributed in other tissues (such as the brain, kidney, and liver), while H has been found only in the skin.[44] In most mammalian tissues, LCBs with 18 carbon atoms predominate, while those with 12 to 28 carbon atoms have been identified in CERs of the SC.[28]

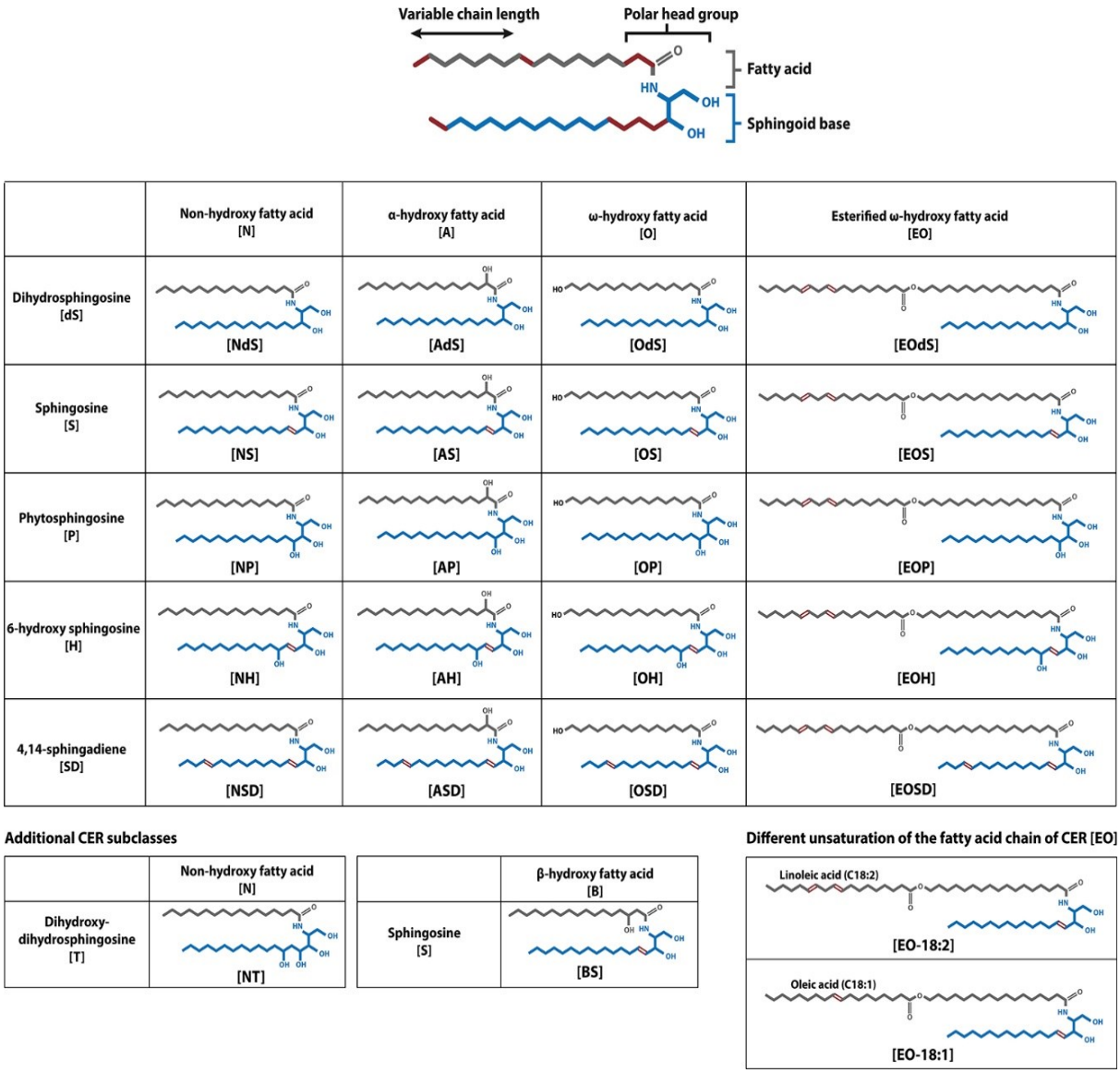

Figure 3. Stratum corneum ceramide subclasses, nomenclature, and structure: Ceramides (CERs) include various subclasses, each composed of a sphingoid base and an acyl chain. The acyl chains can be non-hydroxy (N), α-hydroxy (A), β-hydroxy (B), ω-hydroxy (O), or esterified to linoleic acid (EO). The sphingoid bases include dihydrosphingosine (dS), sphingosine (S), phytosphingosine (P), 6-hydroxysphingosine (H), 4,14-sphingadiene (SD), and dihydroxy-dihydrosphingosine (T). Adapted from "Progress in Lipid Research" journal.[32]

The acyl chain in CERs can be categorized into four types in humans: three non-esterified types, named based on the presence and position of the hydroxyl group, which include non-hydroxy (N), α-hydroxy (A), and ω-hydroxy (O). The fourth type are ω-hydroxy fatty acids that are further esterified, primarily to linoleic acid (EO), and these are known as acyl-ceramides,[43] which are exclusive to the epidermis.[32] Recently, a new type of fatty acid, known as β-hydroxy, was discovered in mouse epidermis, yet their presence in human skin remains unconfirmed. In addition to the mentioned FA types, the SC contains protein-bound ceramides composed of a LCB and a protein-bound ω -hydroxy fatty acid (P-O).[42] FA in ceramides is

usually saturated and unbranched, consisting mostly of either very-long chains (VLCFAs) or ultra-long chains (ULCFAs).[27,28] The chain lengths of acyl chains vary depending on their type. N- and A-type typically have chain lengths ranging from C16 to C30, while O-, EO-, and P-O types generally range from C30 to C36. This variation in chain lengths impacts the functionality of these CERs within the skin's lipid barrier.[42] Sphingolipids with ULCFAs are generally present at very low levels in most tissues. However, they are notably found in the epidermis and spermatogenic cells within the testes.[34]

2.3.3 Nomenclature

Each ceramide class is represented by abbreviations indicating its type of FA and LCB, as initially established by the nomenclature introduced by Motta et al.[45] which was later refined by Robson et al.[46,48]

According to this nomenclature system, each ceramide subclass is represented by a combination of abbreviations indicating the type of FA followed by the type of LCB. The primary 16 subclasses of free ceramides presented in the human epidermis, are denoted as CER NS, CER NdS, CER NP, CER NH, CER AS, CER AdS, CER AP, CER AH, CER OS, CER OdS, CER OP, CER OH, CER EOS, CER EOdS, CER EOP, CER EOH.[49] However, each ceramide subclass encompasses numerous species based on chain lengths and saturation levels, resulting in the identification of over a thousand CER species.[41] Motta et al.'s nomenclature lacks consideration for the lengths of individual chains and the degree of unsaturation. Consequently, a more comprehensive nomenclature system is now employed, encompassing factors such as hydroxylation, chain lengths, and multiple bonds, particularly in mass spectrometry analyses.[42,49] In addition to the classical nomenclature, the number of carbon atoms and double bonds in each chain is indicated in parentheses after the subclass name for each species. For instance, sphingosine with 18 carbon atoms is represented as (d18:1), where the first letter in the notation signifies the count of hydroxyl groups within the LCB (m: mono, d: di, t: tri, or te: tetra), followed by the total carbon atoms in the linear chain, and the final number after the colon indicates the total double bonds within the LCB. Similarly, hydroxylation in the acyl chain is indicated by the letter "h", followed by chain length and the number of double bonds. It's worth noting that for acyl ceramides, the second acyl chain is also denoted the same way. As an illustration, the full nomenclature appears as NS (d18:1,24:0), and EOS (d18:1,h34:0,18:2) in the case of acyl ceramides.[28,42,50]

2.3.4 Biosynthesis

Ceramide formation can occur through three distinct pathways within the appropriate cellular organelles. They can be produced through either the catabolism of sphingomyelin and glycosphingolipids (salvage pathway) or be synthesized through the *de novo* pathway, which involves routes that produce the sphingoid base and the fatty acid.[51] Salvage pathway takes place in the lysosome, where complex glycosphingolipids through a catabolic process via the action of acid ceramidase are converted to Sph. Research indicates that Sph leaves the lysosome and can be either metabolized back into CER or phosphorylated into S1P. On the other hand, Hydrolysis of sphingomyelin (SM) by sphingomyelinases yields CER and phosphocholine. This degradation process occurs rapidly, lasting only a few seconds, in contrast to the *de novo* synthesis of CER, which typically spans several hours.[52]

De novo sphingolipid biosynthesis (**Figure 4**) takes place in the endoplasmic reticulum (ER), initiated with the condensation of L-serine and palmitoyl-CoA, which results in the formation of 3-ketodihydro-Sph (KDS). This rate-limiting step in the entire biosynthesis of sphingolipids is catalyzed by serine palmitoyltransferase (SPTLC1-3) in the presence of pyridoxal 5'-phosphate (PLP) as a co-enzyme. Subsequently, 3-ketodihydro-sphingosine reductase (KDSR), a NADPH-dependent enzyme, reduces this compound to yield dihydrosphingosine.[28,34]

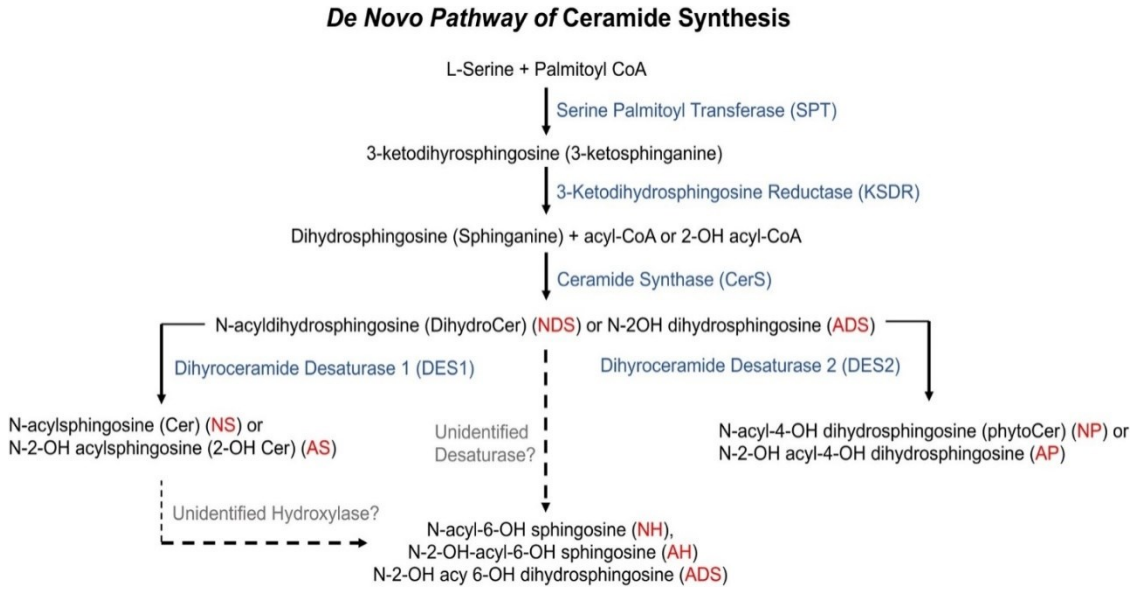

Figure 4. De novo pathway of ceramide synthesis. This schematic illustrates the biochemical steps involved in the de novo synthesis of ceramides, including key enzymes and intermediates. Adapted from the American Journal of Dermatology.[2]

The conversion of dihydrosphingosine to other sphingoid bases does not occur immediately, and it only takes place after the acylation of the primary amino group. The ceramide synthase family (CerS1-6) catalyzes the condensation of acyl-CoA with dihydrosphingosine, leading to the formation of dihydro-CERs. CerS3 is accountable for the creation of epidermal-specific ceramides and is among the enzymes engaged in Acylceramide synthesis.[7,38] Further modification in the polar head of ceramides to form sphingosine and phytosphingosine depends on dihydroceramide desaturases 1 (DEGS1) and 2 (DEGS2), requiring NAD(P)H and oxygen as a cofactor. DEGS1 incorporates a double bond between carbons 4 and 5, catalyzing the generation of Sph-CERs. In contrast, DEGS2 introduces a hydroxy group into position 4 of the carbon chain, making it responsible for the formation of phyto-CERs.[38,40,53] Recently it was discovered that the fatty acid desaturase family protein (FADS3) acts as a ceramide desaturase, producing SD ceramides by desaturating sphingosine-containing CERs.[54] However, enzymes involved in the production of 6-OH CERs remain unidentified.[7,42]

Regarding acyl chains, they originate either from palmitic acid (C16:0) synthesized by fatty acid synthase (FAS) or from LCFAs obtained through diet. Once activated to acyl-CoAs, some of these fatty acids are transformed into VLCFAs and ULCFAs via elongation cycles that take place on the cytosolic side of the ER membrane in keratinocytes. The chain length of acyl-CoA is increased by two at each cycle.[34]

The elongation cycle takes place through 4 steps: condensation, reduction, dehydration, and another reduction. In the first step, starting with condensation of acyl-CoA, by the addition of 2 carbons derived from malonyl-CoA, this rate-limiting step, results in the production of 3-Ketoacyl-CoA. This step is catalyzed by enzymes called fatty acid elongases (ELOVL). ELOVLs exhibit a preference for selected acyl-CoA substrates depending on their hydrocarbon chain length and degree of unsaturation, with seven isoforms identified in mammals (ELOVL1-7). The elongation of VLCFAs involves the engagement of ELOVL6, ELOVL3, ELOVL7, ELOVL1, and ELOVL4.[7,47] ELOVL1 extends the long-chain acyl-CoA to 26 carbons, and biosynthesis of epidermal FAs longer than 26 carbon atoms depends exclusively on ELOVL4.[28,55] The first reduction is catalyzed via 3-ketoacyl-CoA reductase (KAR), using NADPH as a cofactor, followed by dehydration catalyzed by 3-hydroxyacyl-CoA dehydratase (HACD). This is also a rate-limiting step. In the last step, trans-2-enyl-CoA reductase (TER) takes over to catalyze the formation of elongated acyl-CoA.[7,56] The elongation does not only depend on the 4 members of the elongation cycle but also on the type of CerS they appear to complex with.[28]

ULFAs are unique to Acylceramdies and a crucial step after their formation is the hydroxylation at the ω position, which is catalyzed by cytochrome CYP4F22.[47,55] The ultimate stage in the biosynthesis of Acylceramides involves the esterification of linoleic acid (C18:2) at the ω position which is catalyzed by transacylase PNPLA1 (Patatin-like phospholipase domain-containing protein 1) alongside other enzymes.[55] (**Figure 5**)

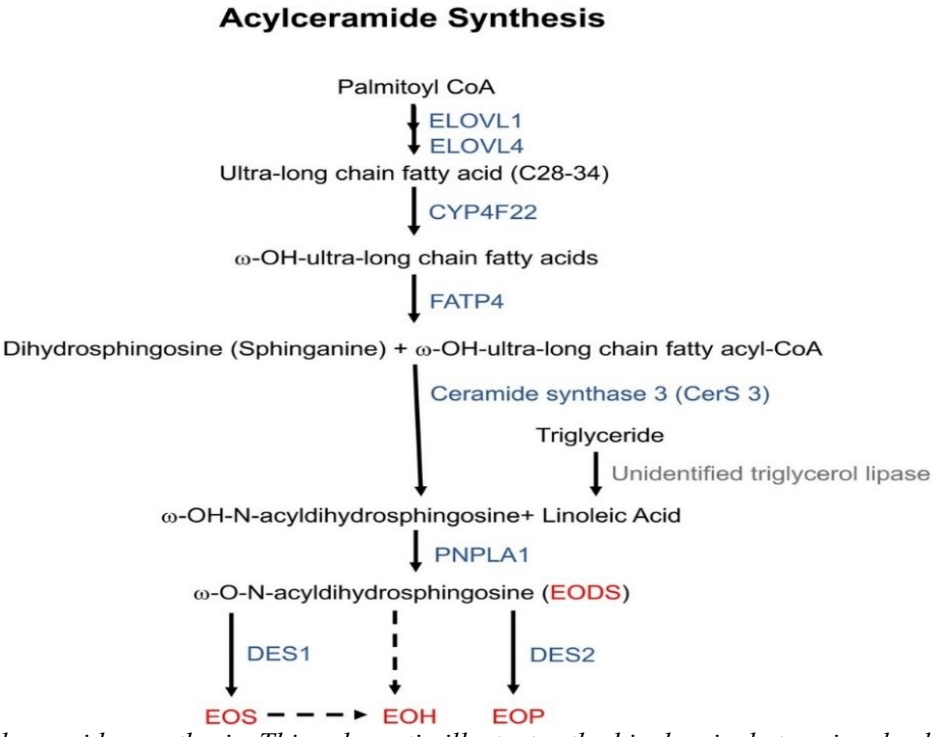

Figure 5. Acylceramides synthesis. This schematic illustrates the biochemical steps involved in the de novo synthesis of ceramides, including key enzymes and intermediates. adapted from the American Journal of Dermatology.[2]

To protect keratinocytes from the cytotoxic effects of CERs, they are rapidly transformed into glucosylceramides (GlcCERs) and sphingomyelins (SMs) in the Golgi apparatus. They are then stored in the LBs and subsequently converted back once they are extruded into the extracellular space. In terms of ceramide subclasses, GlcCER serves as precursors for all types of ceramides, including Acylceramides, whereas CER NS and CER AS originate from SM.[23,28]

The oxygenation by the two lipoxygenases (LOXs) and other hydrolases seems to act as a signal for the esterase-catalyzed hydrolysis of the oxidized linoleic acid, resulting in the production of ω -hydroxy ceramides, which are then crosslinked with CLE.[34,57] Linoleate is essential for the proper functioning of epidermal LOXs and other FAs cannot substitute for it since they are not suitable substrates for these enzymes. In cases where a diet lacks essential fatty acids, linoleate is replaced by other fatty acids like oleate, which interferes with the usual

formation of protein-bound ceramides. This impairment can result in a condition resembling ichthyosis, which includes symptoms like dermatitis and increased TEWL.[14,58]

2.3.5 Quantification of Ceramides in the Stratum Corneum

Tape stripping is a valuable technique for obtaining SC samples. When combined with other analytical techniques such as spectrometry or chromatography, tape stripping becomes a powerful tool for analyzing and quantifying lipids in the SC.[6] Throughout history, initially, five classes of ceramides were identified using TLC (thin-layer chromatography), Gas chromatography (GC), and NMR (nuclear magnetic resonance).[59] Later, through the utilization of HPTLC (high-performance thin-layer chromatography) in combination with NMR and GC, more subclasses were identified.[60] TLC and HPTLC continue to be fundamental tools in modern analytical chemistry. HPTLC is valued due to its speed and cost-effectiveness for the separation of complex mixtures.[45,46,61,62] This method is particularly suitable for smaller nonpolar compounds and provides certain benefits over high-performance liquid chromatography (HPLC).[63] However, the utilization of TLC and HPTLC plates may pose challenges in identifying isolated fractions due to the simultaneous appearance of multiple ceramides at the same spot, such as CER AS and CER NdS.[32]

Technological advancements in LC/MS methods (Liquid chromatography-mass spectrometry) further facilitated the identification of additional subclasses as well as individual species of CERs.[32,64] LC/MS provides comprehensive details on lipid subclasses and the distribution of chain lengths within each subclass, a level of analysis that is not achievable with the traditional TLC technique.[65] Additionally, switching from TLC to HPLC and coupling with a mass spectrometry (MS) detector, which measures the mass-to-charge ratio, increases the capacity for examining altered lipid patterns in skin diseases like psoriasis and atopic dermatitis.[66] Before performing MS analysis of skin ceramides, it is essential to separate them using LC, which can be accomplished through either normal phase (NPLC) or reverse phase chromatography (RPLC).[67-70] RPLC differentiates ceramides based on their hydrophobic properties, which depend on the chain length and the number of double bonds in both the FA and the LCB. Conversely, NPLC separates ceramides based on their hydrophilic properties, specifically the polar head structure. However, using RPLC can greatly enhance the efficiency of ceramide separation, similar to the advancements made in phospholipid analysis.[71] This is attributed to the substantial hydrophobic nature of ceramides.[41]

Today, for enhanced precision in detecting and quantifying specific lipid molecules, the LC/MS/MS method (liquid chromatography with tandem mass spectrometry) in the MRM

mode (multiple reaction monitoring) is utilized. This technique tracks the transition of a selected precursor ion to its specific product ion through collision-induced dissociation.[43]

In alignment with findings from prior research,[41,64] Kawana. et. al.[43] utilizing LC/MS/MS with MMR, demonstrated that CER NP, NH, and AH are the most abundant in the human SC, comprising respectively 24.2%, 23.7%, and 18.0% of total CERs. Subsequently, AP, NdS, NS, AS, EOH, EOS, EOP, and AdS follow in descending order (ranging from 9% to 1%). Other CER classes are present in proportions lower than 1%. Regarding LCBs, 6-hydroxy-Sph, and Phyto-Sph ceramides are notably abundant in the human SC accounting for 45.4% and 34.7%, respectively, followed by S and dS. In terms of the acyl chain, the non-hydroxy ceramide class holds the highest proportion, followed by α-hydroxy ceramides, EO ceramides, and ω-hydroxy ceramides, constituting 59.4%, 32.5%, 6.3%, and 1.6%, respectively.

The composition of SC ceramide classes differs significantly between humans and mice. In the mouse SC, NS levels are the highest (57.9% of total ceramides), followed by EOS, NdS, OS, and BS in descending order (16% to 4%). The proportions of other ceramide classes are lower than 2%. Additionally, in mice, the EO, ω -hydroxy, and β -hydroxy ceramide classes account respectively for 16.9%, 8.7%, and 4.9%, while α-hydroxy ceramide, the second-highest ceramide class in humans, is quite low (0.7%).[42,43]

It is noteworthy that ceramides with odd-numbered FAs are typically present at low levels in most tissues. However, in both human and mouse SC, ceramides with odd-chain FAs, like C25, C27, C29, and C31, are found in relatively high levels, making up about 21–23% and 6–10% of the total ceramide content, respectively.[26,43]

2.4 Importance of Stratum Corneum lipids in skin diseases

Several skin diseases are associated with abnormalities in the barrier function of the SC, and importantly alteration in the lipid composition and organization of the intercellular matrix. It has been shown that these changes include alterations in the CER:CHOL:FFA ratio, and FFA chain lengths, as well as changes in CER composition, and length and degree of unsaturation of their acyl chains. CERs play a crucial role in maintaining the structure of the SC and regulating skin barrier homeostasis. They have a significant impact on the water retention properties and barrier function of the SC. Thus, alterations in ceramide levels can result in dry skin and compromised barrier function, potentially contributing to the development of skin diseases. In addition, CERs function as active second messengers, regulating keratinocyte proliferation and differentiation, boosting the production of pro-inflammatory cytokines, and modulating immune responses. The disrupted metabolism and function of ceramides are

implicated in the development of several inflammatory skin diseases, including PSO, AD, and ichthyosis. Given the complexity of epidermal lipid composition, influenced by numerous external and internal factors, identifying which factors contribute most to the reduced barrier function and determining the best treatment remains a significant challenge.[26,40,72]

2.5 Psoriasis

Psoriasis is a non-infectious skin disease characterized as an immune-mediated chronic inflammatory disorder with a significant genetic predisposition, often accompanied by other systemic comorbidities. The global prevalence is estimated at around 2%, though it differs across regions. There are different clinical subtypes, with Psoriasis Vulgaris, also referred to as chronic plaque-type psoriasis, being the most prevalent, accounting for roughly 90% of cases. Other subtypes include Inverse Psoriasis, Guttate Psoriasis, and Pustular Psoriasis. The defining feature of psoriasis is persistent inflammation, resulting in hyperproliferation and thickening of the epidermis, known as acanthosis, and uncomplete differentiation of keratinocytes resulting in abnormal retention of nuclei in the SC, known as parakeratosis. The typical clinical signs are well-defined as reddish itchy plaques topped with silvery scales. These plaques can merge to cover extensive skin areas and are commonly found on the trunk, limbs, and scalp. Typically manifesting in the skin, psoriasis can also impact joints and is associated with various other diseases. Furthermore, with inflammation extending beyond the skin, psoriasis might affect multiple organs and is believed to increase the risk of cardiovascular conditions like hyperlipidemia, hypertension, coronary heart disease, and type 2 diabetes mellitus.[73]

Approximately 70% to 80% of individuals with psoriasis have mild to moderate forms of the condition, which can be effectively managed using topical treatments. Conversely, moderate to severe cases often necessitate treatments such as UV therapy, oral medications, or biological therapies.[74]

2.5.1 Sphingolipid pathogenesis in psoriasis

It has long been reported that psoriatic skin exhibits compromised epidermal barrier integrity and disrupted ceramide metabolism. Motta et al.[45] were the first to observe alterations in ceramide content within the SC. Additionally, they observed increased TEWL and a decreased ratio of FFAs to the total lipid content in the psoriatic scale. Despite these changes, they stated that the total amount of CERs remained the same. More studies considering the difference between lesional and non-lesional areas have shown a decrease in the level of

ceramides in the lesional skin compared to non-lesional. However, the amount of ceramide in the non-lesional skin of patients with PSO is only slightly decreased compared to healthy skin. Nonetheless, at the level of mRNA and enzyme levels of β-glucocerebrosidase, a decrease was noted in the psoriatic epidermis, although, its level is higher in lesional compared to non-lesional psoriatic skin. Additionally, there is a decrease in the level of SMase in the lesional skin compared to non-lesional.[75-82]

Regarding the alteration in CER *de novo* synthesis, there is a significant decrease in protein expression of the SPT enzyme in lesional compared to non-lesional skin.[83] The diminished levels of both CER and the SPT enzyme exhibit an inverse correlation with the PASI score (Psoriasis Area and Severity Index), which is used to assess the severity of plaque psoriasis in mild to moderate form.[84] In the analysis using mass spectrometry, Tawada et al.[85] observed that the proportion of CERs containing ULCFA was notably lower in patients with AD and PSO compared to healthy individuals. Moreover, this reduction was more pronounced in PSO patients compared to those with AD. Interestingly, among various cytokines examined, interferon-gamma (IFN-γ), known to be abundant in psoriatic skin, decreases the mRNA expression of ELOVL 1 and 4 and CerS 3 enzymes. As both of these enzymes are involved in synthesizing and elongating the acyl chain of CERs, this finding may elucidate the reduction of ULC CERs and the increase in VLC CERs in psoriatic skin. This shift in the length of the acyl chain results in the alteration of lipid organization and phase separation in extracellular lipid membranes.[72,85]

Recent studies found that in human psoriatic lesions, the levels of two LCBs, sphingosine and dihydrosphingosine, are significantly higher compared to non-lesional skin. Additionally, the percentage change in ceramidase protein expression shows a significant positive correlation with the PASI score.[86] Patients with PSO exhibit elevated levels of S1P compared to healthy individuals. Moreover, research has shown that the quantity of S1P in psoriatic patients varies based on the patient's weight. In keratinocytes, S1P activates the pathway of expression of various pro-inflammatory genes, which supports the importance of CER degradation in the progression of PSO.[87]

While the CER NS levels are elevated, Phyto-CERs (such as CER NP and CER AP), as well as Acylceramides, are both reduced in psoriatic lesions. This reduction correlates with increased TEWL and inferior water retention capacity. Phyto-CERs enhance the structural integrity of the SC barrier by forming robust hydrogen bonds and highly stable domains within the extracellular lipid matrix. Decreased levels of Phyto-CERs and Acylceramides, crucial components for the structure of epidermal lipid lamellae and keratinocyte differentiation, are

implicated as causal factors in permeability barrier dysfunction and hyperproliferation in PSO.[72] Another recent study revealed that the ratios of NP/NS, NH/NS, NP/AS, NH/NS, NDS/AS, ceramide AH/AS, and ceramide EOP/AS are lower in psoriatic skin, particularly in lesional areas compared to non-lesional skin.[2]

Topical treatments like moisturizers with ceramides and keratolytic agents have shown effectiveness in the improvement of PSO. Products containing CERs may improve barrier function, reducing TEWL, and maintaining skin hydration. Patients responded well to their aesthetic attributes and overall performance, with improvements in skin health.[1]

2.5.2 Imiquimod-induced psoriasis (IMQ-P)

Dendritic cells serving as antigen-presenting cells are known to be important players in the initial stages of the disease. In humans, two types of dendritic cell subsets have been recognized: myeloid DCs (mDCs) and plasmacytoid DCs (pDCs). One proposed mechanism involves the recognition of antimicrobial peptides (AMPs) such as LL37, which are abundantly secreted by keratinocytes in response to injury and are notably overexpressed in psoriatic skin. LL37 protein binds to RNA and stimulates toll-like receptors 7 and 8 (TLR7, TLR8, respectively) on mDC and pDC starting an immune response pathway leading to the progression of psoriasis.[73]

Imiquimod, an agonist of TLR-7, is an immunotherapy drug used for treating various skin conditions. It is also known to induce psoriasis or psoriasis-like lesions (IMQ-p).[88] Imiquimod is by far the most widely used acute mouse model for studying psoriasis-like skin inflammation. Applying topical imiquimod to the mouse ear or back skin produces a phenotype that shares many characteristics with humans. The strengths of the approach include its ease of use, convenience, low cost, and the ability to induce an acute inflammatory response. However, it also has several limitations, such as unintended systemic effects from topical treatments, overuse without sufficient validation studies, unclear mechanisms of action, potential observer bias, histological misinterpretation, and a limited ability to replicate all aspects of human psoriasis.[89]

3. MATERIALS AND METHODS

3.1 Sampling and measurement of Transepidermal water loss

The experimental protocols were carried out in strict adherence to ethical guidelines aimed at minimizing animal use and alleviating their suffering. Sampling and TEWL measurements were conducted by our collaborator, Michal Korinek, at the College of Medicine, Chang Gung University, Taoyuan, Taiwan.

Seven-week-old BALB/c white female mice (weighing approximately 20 g) were housed in an air-conditioned room with a 12-hour light-dark cycle. On the first day, the hair on the back of each mouse was shaved with a razor, followed by the application of hair removal cream. After 10 to 15 minutes, the hair removal cream was thoroughly washed off to ensure complete removal of the hair. Twelve mice were randomly divided into four groups, with each group containing three mice, for the treatment protocols. The control group received no treatment. To induce psoriasis-like symptoms, a dose of 62.5 mg of a 5% w/w Imiquimod (IMQ) cream (Aldara, 3M Health Care Limited, Loughborough, United Kingdom) was applied to the dorsal side of the mice daily for five consecutive days. The second group received only IMQ. The third group was treated with IMQ and a blank cream (Solidified Animal Fat 0.15%, Cetyl Alcohol 0.55%, Stearic Acid 0.09%, Cholesterol 0.08%, Polysorbate 80 0.30%, Glycerol Monostearate 0.15%, Refined Sunflower Oil 0.20%, 1,3-Propandiol 0.50%, Glycerol 85% 0.50%, and Sodium Acetate Solution with Acetic Acid adjusted to pH 5.5.), while the fourth group received IMQ along with ceramide EOS29 0.5% cream (20 mg in 4 g of cream) combined with blank cream. The amount of EOS29 cream applied was 80 mg/mouse per day. The application area for all creams was 2 × 1 cm.

Obtaining stratum corneum samples from mouse skin was performed using tape-stripping with a 22-mm diameter D-squame tape, which consists of an adhesive part for sample collection and a non-adhesive part for handling. The tape was applied to the dorsal area of the mice. Eight samples were collected from each mouse, all from the same spot, to ensure consistency in the analysis. In addition to these eight samples, two control strips, which were not used for analysis, were also included. Thus, a total of ten tapes were obtained from each mouse.

The Tewameter® (Courage & Khazawa, Cologne, Germany) was employed to assess skin hydration within a controlled, moisture-proof environment to prevent inaccuracies due to atmospheric changes. The probe was positioned on the mouse's back and pressed against the skin to measure moisture loss from the stratum corneum. Each measurement was conducted

for 30 seconds, during which relative humidity and temperature fluctuations were monitored to ensure a stable reading. Measurements were repeated daily for a total of four days. The average result was reported as water dispersion, with units of g/m²/h.

3.2 Measurement of protein content

After removing the strips from the Eppendorf tubes, the samples were transferred to a plastic holder with round mouth. The protein content was then measured using a SquameScan instrument (Heiland electronic GmbH, Wetzlar, Germany), which evaluates optical absorption in the infrared region (850 nm) and is specifically designed for this application. Prior to measurement, the device was calibrated to a reference value with a permissible deviation of 0.3. A control tape without a skin sample was used as a reference sample before measuring the actual samples. Consistent time intervals were maintained between measuring and recording the values of individual samples.

After measurement, the samples were transferred from the holder to 15 ml glass centrifuge tubes with the sticky side containing the sample facing inward. Samples in the form of pairs from individual mice were placed in each test tube, resulting in samples No. 1+2, 3+4, 5+6, and 7+8, thereby generating four test tubes per mouse. The strips were inserted into the tubes as low as possible to avoid overlap.

3.3 Lipid Extraction

100 µL of internal standard and 8 mL of a solvent mixture (chloroform/methanol/water in a 30:60:8 ratio) were added to the SC sample tubes, and the samples were left on a shaker overnight at room temperature. After shaking, the tubes were centrifuged at 3500 rpm for 10 minutes. The resulting supernatant containing lipids was transferred to a new test tube and partially evaporated using a stream of nitrogen at a temperature of 43°C. A new 7 mL of the same solvent was added to the remaining biological material in the first tube containing the discs, and the entire contents were placed in an ultrasonic bath for 3 minutes at 45°C. After three minutes, the sample was left in the water bath for another 12 minutes at the same temperature. The tube was again centrifuged at 3500 rpm for 10 minutes, and approximately 7 mL of the supernatant was withdrawn with a syringe and added to the second tube for evaporation. The tubes with the remaining discs were stored in a freezer in case covalently bound lipids were quantified in the future. The contents of the second test tube were evaporated to dryness under a stream of nitrogen, resulting in a white coating on the tip of the test tube.

1.5 mL of solvent (chloroform/methanol in a 1:9 ratio) was added to the tube, which was then placed in an ultrasonic bath for about 30 seconds at room temperature and vigorously mixed. The contents of the tube were withdrawn using a plastic syringe (2 mL) with a long cannula and filtered through a filter (PTFE, diameter 13 mm, pores 0.2 μm) into a 1.5 mL vial. This final sample was stored in a freezer until LCMS measurement. For measurement, it was preferable to transfer 250 μL of this sample to another vial containing an insert, rather than using the entire amount.

3.4 Separation and quantification of ceramides

The obtained ceramide fractions were analyzed using high-performance liquid chromatography (HPLC) coupled with mass spectrometric detection (HPLC-MS/MS) on a triple quadrupole LCMS-8050 instrument (Shimadzu Prominence, Kyoto, Japan). Sample ionization was performed by electrospray ionization (ESI) in positive mode.

Ceramide separation was achieved on a C18 reverse-phase column with a gradient elution of the mobile phase B, ranging from 43-99% (A: 50% methanol, 50% water, 0.1% formic acid, and 10 mM ammonium formate; B: 99% isopropanol, 1% methanol, 0.1% formic acid, and 10 mM ammonium formate). The analysis duration was 32 minutes, with a mobile phase flow rate of 0.2 mL/min. Reverse-phase separation was conducted on a 15 cm × 2.1 mm Ascentis chromatographic column with 3 μm particle size (Supelco, Bellefonte, PA, USA) at 30°C. A 3 μL sample was injected into the column.

Detection was performed using a QqQ MS (LCMS-8050). The mass spectrometer parameters were set as follows: nebulization gas at 3 L/min, drying gas at 10 L/min, heating gas at 10 L/min, source temperature at 300°C, desolvation line temperature at 250°C, heated block temperature at 400°C, source voltage at 4 kV, and collision gas pressure at 270 kPa. Measurements were conducted in MRM (multi-reaction monitoring) mode.

3.4.1 Preparation of Internal Standard

The internal standard preparation included ceramides NS (18:1/14:0), NS (18:1/19:0), NS (18:1/31:0), NdS (18:0/14:0), NP (18:0/14:0), EOS-d7 (18:1(d7)/32:0, 18:2), and base S (14:1), dS (17:0). Individual ceramide components were dissolved in a chloroform/methanol mixture ($CHCl_3$:MeOH in the ratio of 1:9) and subsequently diluted with pure methanol to achieve a final concentration of 20 μmol/L.

After diluting the individual ceramides, 50 μl of each ceramide/base solution was mixed together and filled up with MeOH in a single tube to adjust 5 ml, resulting in a final internal

standard concentration of 200 nmol/L (2nmol/10ml) A 100 µL of this internal standard was added to each sample, yielding a final concentration of 20 pmol/sample. This concentration was used for the subsequent calculations in the quantification of ceramides.

3.4.2 Preparation of External Standard

The prepared external standard comprised the following ceramides: NS (18:1/24:0), NdS (18:0/24:0), NP (18:0/24:0), EOS (18:1/32:0/18:2), EOdS (18:0/32:0/18:2), AS (18:1/24:0), AdS (18:0/24:0), AP (18:0/24:0), NH (18:1/24:0), OS (18:1/32:0), OdS (18:0/32:0), OP (18:0/32:0), S base (18:1), dS (18:0), and P (18:0). The preparation process for the external standard was identical to that of the internal standard, resulting in a final concentration of 200 nmol/L.

3.5 Data Processing

Data from LC-MS/MS analyses were acquired using LabSolutions software (version 5.96), which facilitated chromatogram modifications and the application of curve smoothing through the Sawitzky-Golay method. Peak area data were subsequently transferred to Microsoft Excel for mathematical corrections, including quantification via internal and external standards, adjustment of detector response relative to chain length, and protein content calculations. Final graphical representations and statistical analyses were conducted using GraphPad Prism 9.

3.6 Statistical Analysis

Statistical data analysis was conducted using ANOVA for grouped comparisons, followed by Tukey's post hoc test. Results are expressed as mean ± standard error of the mean (SEM). Statistical significance was assessed with p-values as follows: * $p < 0.05$; ** $p < 0.01$; *** $p < 0.001$; **** $p < 0.0001$

4. RESULTS AND DISCUSSION

4.1 Experimental Design

For the experiment, 12 subjects were randomly assigned into four groups, each consisting of 3 mice, based on the treatment regimen they received. The first group served as the control and received no treatment, the second group was administered Imiquimod to induce psoriasis, the third group received Imiquimod along with a blank cream, and the fourth group was treated with Imiquimod in combination with ceramide EOS29 cream. For easier reference, these groups will hereafter be mentioned as Control, IMQ, IMQ+Blank, and IMQ+EOS, respectively. From each mouse, ten strip tapes were obtained from the same spot.

Eight of these strips were subsequently combined into four pairs (1+2, 3+4, 5+6, and 7+8) for further measurements and analysis. In addition to these eight stripes prepared for experimental purposes, two strips were reserved and were not subjected to any experimental procedures. Sampling and initial experiments were conducted by our collaborators at Chang Gung University College of Medicine in Taiwan. They also measured transepidermal water loss and subsequently sent us the tape strips. We then performed lipid extraction and analysis on the received samples. Among other aspects, we determined the protein content in the stratum corneum and quantified the total ceramide content for each ceramide subclass in the SC using LC-MS/MS. Our specific focus was on analyzing ceramide profiles in the SC, determining their average acyl chain length, and evaluating the ratio between very long and ultra-long chain ceramides.

4.2 Transepidermal water loss

Transepidermal water loss (TEWL) is a critical dermatological indicator of skin barrier function, reflecting the skin's capacity to regenerate following damage. TEWL measurements, conducted by our collaborators, were recorded daily for four days prior to skin stripping to establish baseline values (**Figure 6**, **left**). Increased TEWL was observed in all treatment groups compared to the control, with the IMQ+EOS group exhibiting the highest TEWL on the fourth day of measurement. Following stratum corneum (SC) sampling, TEWL was measured approximately hourly for three hours to assess the skin's recovery and compensate for damage caused by the collection process (**Figure 6**, **right**). TEWL was elevated in all treatment groups compared to the control, with the IMQ+EOS group showing the greatest increase. This was followed by the IMQ+Blank group, while the IMQ group exhibited the smallest increase among the treatment groups. A compromised skin barrier and elevated TEWL

are characteristic of many skin disorders, including psoriasis. In psoriasis, increased TEWL and diminished water retention capacity are frequently observed, attributable to disrupted ceramide levels. These clinical manifestations are indicative of impaired barrier function.[1]

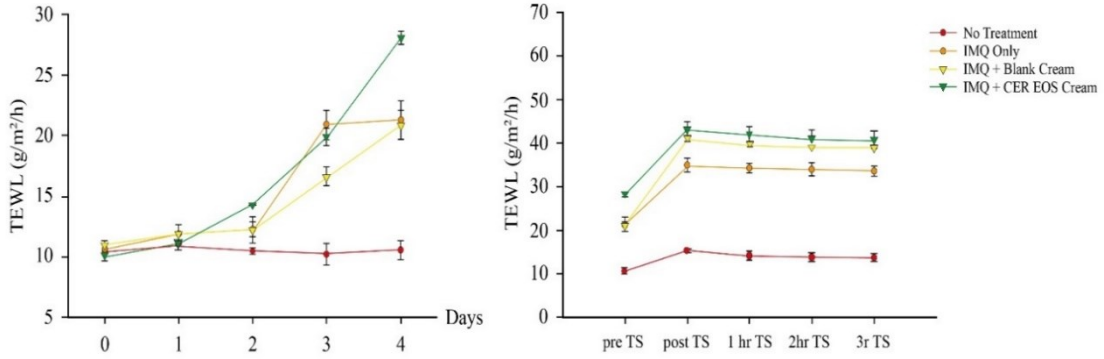

Figure 6. Transdermal water loss measurement results. On the left: daily measurement of TEWL before tape stripping. On the right: measurement of TEWL after SC sampling. Data are shown as mean (± SEM, n =3)

4.3 Determination of protein content

First, the protein content of the D-squame strips collected from individual subjects was determined. This step was crucial because, despite the D-squame patches being designed for this application, the amount of stratum corneum sample collected could vary.

As depicted in **Figure 7**, the IMQ+Blank group demonstrated a statistically significant increase in protein content compared to both the control and IMQ+EOS groups. Furthermore, although one mouse in the IMQ group exhibited an increase in protein content, this observation was not replicated in the other two mice within the same group.

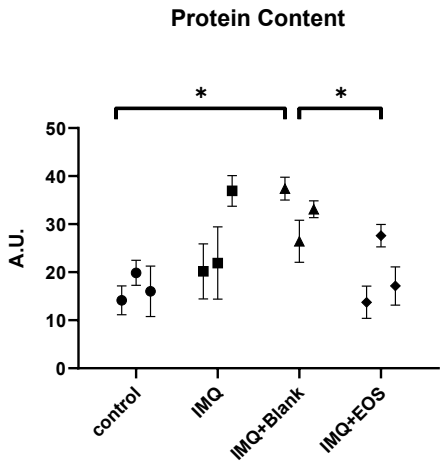

Figure 7. Protein content in individual mice was quantified using the SquameScan device. Data are shown as mean (± SEM, n =3). Asterisks: p < 0.05 (*)

The protein content serves as an indicator of certain skin properties, such as cohesion, but in this case, it was primarily measured to enable direct comparisons between individual patches. In the future, a detailed analysis of the samples could be highly informative. Such an analysis would reveal specific proteins whose quantities vary significantly in the samples, such as filaggrin, involucrin, loricrin, or keratins. Identifying these variations could provide deeper insights into skin health and disease mechanisms.

4.4 Total ceramide content

The combination of reverse-phase HPLC with triple quadrupole mass spectrometer detection allows for the separation of individual ceramide molecules within a subclass based on differences in their chain lengths. The retention time increases with increasing chain lengths. For this project, only ceramides containing a sphingoid base of length 18C were analyzed, despite the presence of sphingoid bases with other chain lengths in mouse SC. Including these would have disproportionately increased the volume of measured data. The triple quadrupole mass spectrometer enables targeted detection and quantification of individual molecules based on their specific transitions between precursor and product ions (in our case, in positive ionization mode). Using the MRM (multiple reaction monitoring) technique, we can monitor a large number of these transitions simultaneously.

The graph depicted in **Figure 8** (**left**) illustrates the total levels of all ceramide subclasses and their respective acyl chain lengths, with the exception of CER EOS29. Given that the cream applied contained CER EOS29, it was necessary to exclude this particular ceramide from the analytical assessment to ensure the accuracy of the results. CER EOS29 was detected exclusively in the IMQ+EOS group, with its levels being significantly higher compared to those in the other treatment groups, where CER EOS29 was undetectable. (**Figure 8**, **right**) To accurately evaluate the effects of the applied cream, EOS29 was omitted from the subsequent analyses. The measurement results are shown on the y-axis as the amount of picomoles per sample, divided by a unit of protein content. This unit was used for standardization to ensure that lipids were always measured from the same amount, thereby preventing distortion of results due to varying collection yields between samples. It is also possible to quantify the total content of ceramides without considering the protein content, resulting in the amount of ceramides per patch. However, this method carries a significant risk of variability in sample collection, potentially distorting the results. Therefore, in the subsequent sections of this work, the results will always be presented after normalization for protein content.

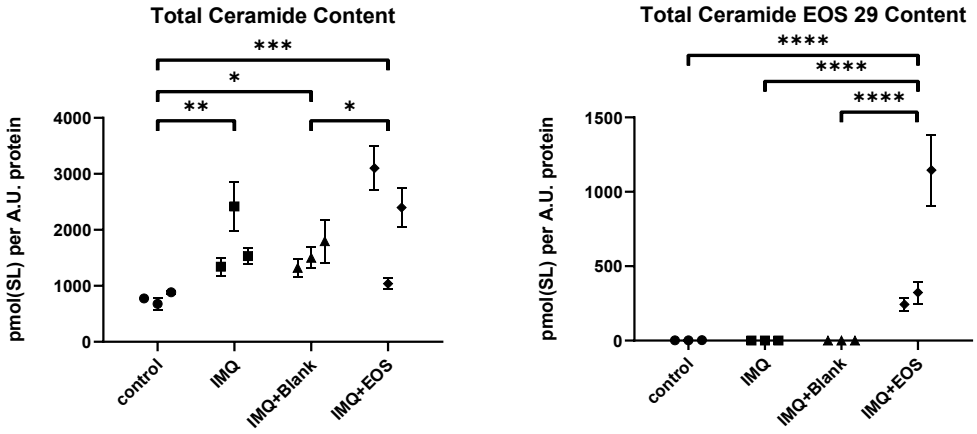

Figure 8. On the left: The total content of ceramides. On the right: Total content of CER EOS29 which was applied in the cream only in the IMQ+EOS group. Data are shown as mean (± SEM, n =3). Asterisks: p < 0.05 (*), p < 0.01 (**), p < 0.001 (***),p < 0.0001 (****)

Alterations in overall ceramide levels have been documented in various skin diseases, including psoriasis. Previous research indicates that ceramide synthesis is significantly reduced in the lesional epidermis, showing an inverse correlation with clinical severity in mild to moderate psoriasis. Additionally, the decrease in both ceramide synthesis and its levels in keratinocytes is positively correlated with the PASI score.[77,78] However, studies have shown variability in total ceramide levels in the stratum corneum; some have found unchanged levels of total ceramides in psoriatic lesions compared to healthy human SC.[45,90] This highlights the complex role of ceramides in psoriasis, specifically in the context of induced psoriasis as investigated in our experiment. Additionally, the IMQ+EOS group showed an even more pronounced increase compared to the other treatment groups.

4.4.1 Overview of the total content of ceramides based on their acyl chain

Prior to discussing each ceramide subclass in detail, we analyzed the total ceramide content categorized by their fatty acid compositions shown in **Figure 9** to provide a comprehensive overview.

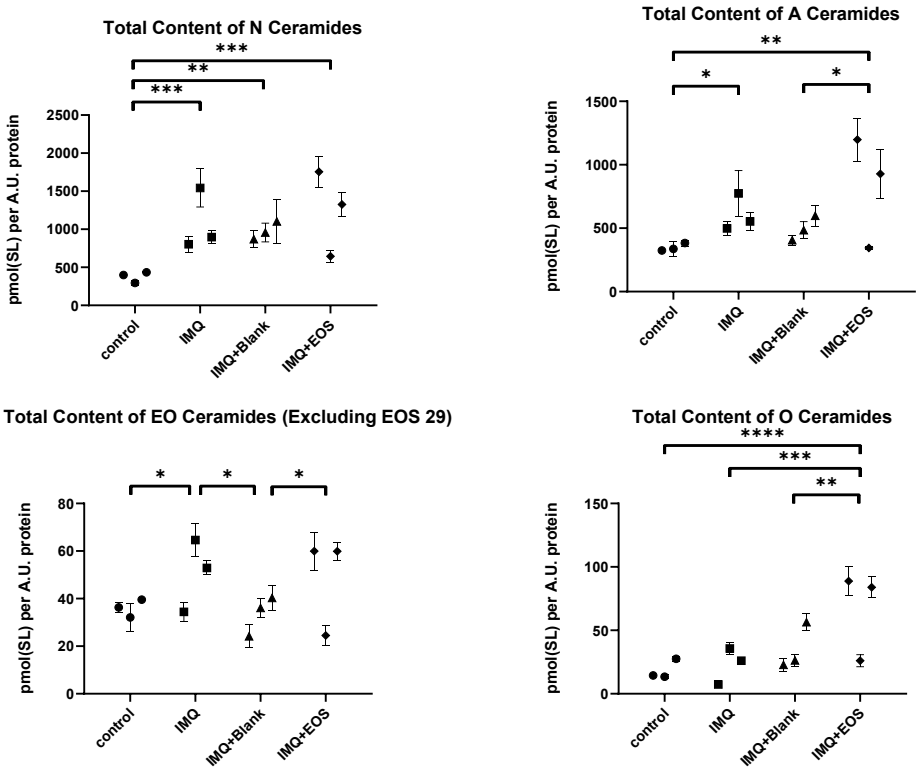

Figure 9. The total content of ceramides which are classified based on their fatty acid chain. Data are shown as mean (± SEM, n =3). Asterisks: p < 0.05 (*), p < 0.01 (**), p < 0.001 (***)

The total content of non-hydroxy ceramides (N) increased across all treatment groups compared to the control, with no significant difference among the treatment groups themselves. For α-hydroxylated ceramides (A), we also observed an increasing trend among treatment groups compared to the control. However, for the IMQ+Blank group, this increase was not statistically significant. Notably, the IMQ+EOS group exhibited the most pronounced rise among the treatment groups. For ω-esterified ceramides (EO), although differences were detected among the treatment groups, further investigation of each subclass is required to discuss these differences in detail. For ω-hydroxy ceramides (O), an increase was observed only in the IMQ+EOS group, which exhibited a significant difference compared to the other groups, including the control.

4.4.2 Overview of the total content of ceramides based on their sphingoid base

Similar to the previous section, here we analyzed the total ceramide content categorized by their sphingoid bases. As it is shown in **Figure 10**, the total content of both sphingosine-containing ceramides and phytosphingosine ceramides was increased. In previous studies, it was observed that the amounts of sphingosine and dihydrosphingosine are significantly elevated in psoriatic epidermis compared to non-lesional epidermis.[86] Our findings are

consistent with these results. Motta et al.[45] and Choi et al.[40] characterized psoriasis by a significant reduction in the proportion of phytosphingosine-carrying ceramides in comparison to normal SC. It has been reported that in psoriatic scales, these ceramides constitute 25% of the total ceramide content, whereas in normal SC, they represent 44%.[1] Interestingly, we observed the opposite result across all our treatment groups compared to the control.

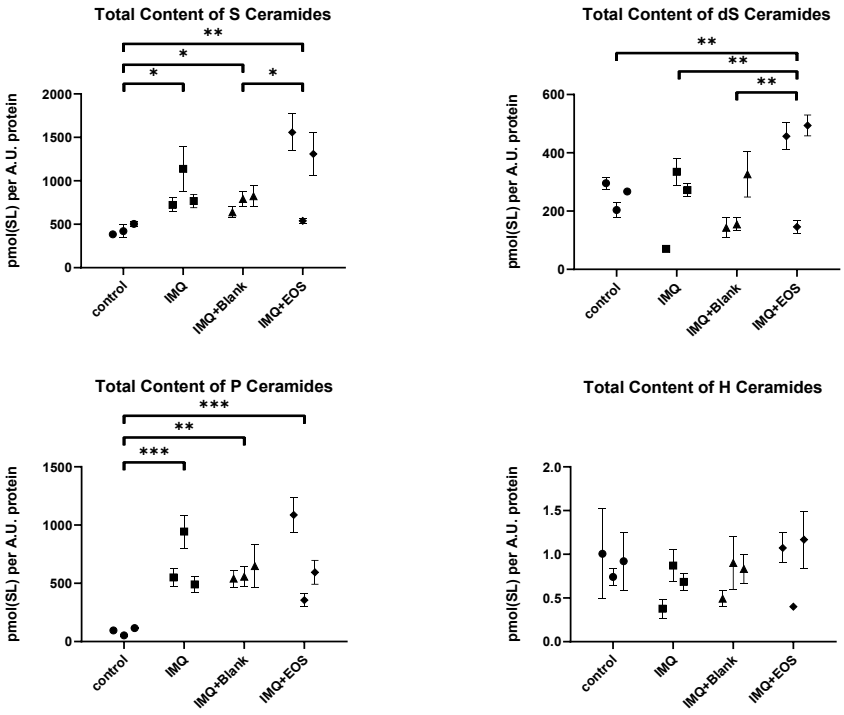

Figure 10. The total content of ceramides which are classified based on their long-chain bases. Data are shown as mean (± SEM, n =3). Asterisks: p < 0.05 (*), p < 0.01 (**), p < 0.001 (***)

In the following sections, we will further discuss the details concerning each ceramide subclass and more specifically the changes regarding Phyto-CERs.

As anticipated and demonstrated in previous studies,[43] 6-hydroxy sphingosine-carrying ceramides NH, AH, EOH, and OH are present at very low, almost undetectable levels in mouse SC, in contrast to their higher levels in human SC. In the subsequent sections, we have included their levels in the figures for illustrative purposes; however, we will not discuss them further, as they hold no significant relevance in the mouse SC.

4.5 Quantification of Non-hydroxylated ceramides (N)

For each subclass of N ceramides, the total levels were calculated by summing all determined chain lengths, which include the C18 sphingoid base along with acyl chain lengths ranging from 16 to 32 carbons.

4.5.1 Total content of Non-hydroxylated ceramides (N)

Previous studies have shown that the levels of ceramide NS and NdS are elevated in psoriatic lesions in both human SC and mouse models. These studies also reported a reduction in ceramide NP levels.[45,72,90] Other investigations found that keratinocytes within psoriatic lesions displayed increased levels of both ceramide NS and ceramide NP.[91]

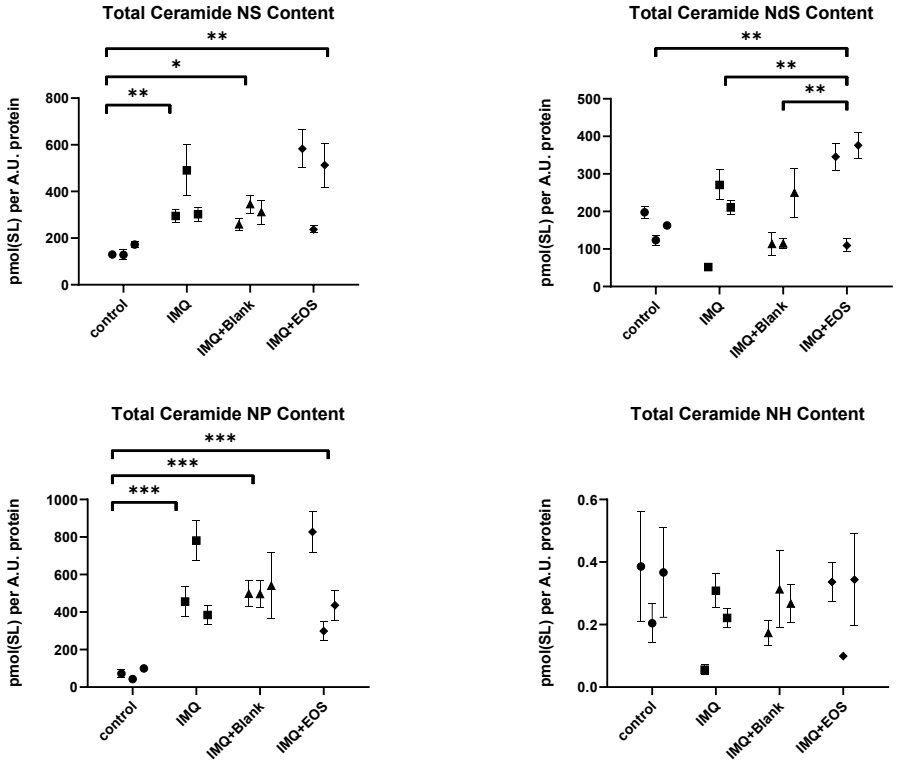

Figure 11. Quantification of non-hydroxylated ceramides. Data are shown as mean (± SEM, n =3). Asterisks: p < 0.05 (*), p < 0.01 (**), p < 0.001 (***)

In this study, the analysis of ceramide NS showed an increasing trend in all treatment groups compared to the control group, aligning with previous findings. For ceramide NdS, an increase was observed only in the IMQ+EOS group compared to the other groups, including the control. Interestingly, we observed an increasing trend for ceramide NP among all treatment groups and control, which correlated with TEWL, contrasting with some previous studies.

The work of Školová et al. reported that model membranes containing phytosphingosine ceramide NP24 exhibited markedly higher permeability compared to those containing sphingosine ceramide NS24 and dihydrosphingosine ceramide NdS24. This increased membrane permeability was linked to the unsaturation or C4-hydroxylation of dihydroceramides, which are associated with a deterioration in the skin's barrier function.[91]

This observation partially elucidates the correlation between elevated levels of NP ceramides and increased TEWL, suggesting that Phyto-CERs may play a significant role in modulating skin barrier permeability.

4.5.2 Average acyl chain lengths of Non-hydroxylated ceramides (N)

Multiple studies have established a correlation between the acyl chain length in ceramides and membrane permeability. It has been demonstrated that short-chain ceramides increase the permeability of model membranes.[93] Additionally, it has been observed that IFN-γ, which is prevalent in psoriatic lesions, reduces the levels of ceramides with long-chain fatty acids by downregulating elongation of very long-chain fatty acids and CerS3. This mechanism may contribute to the altered ceramide profile observed in psoriasis.[85]

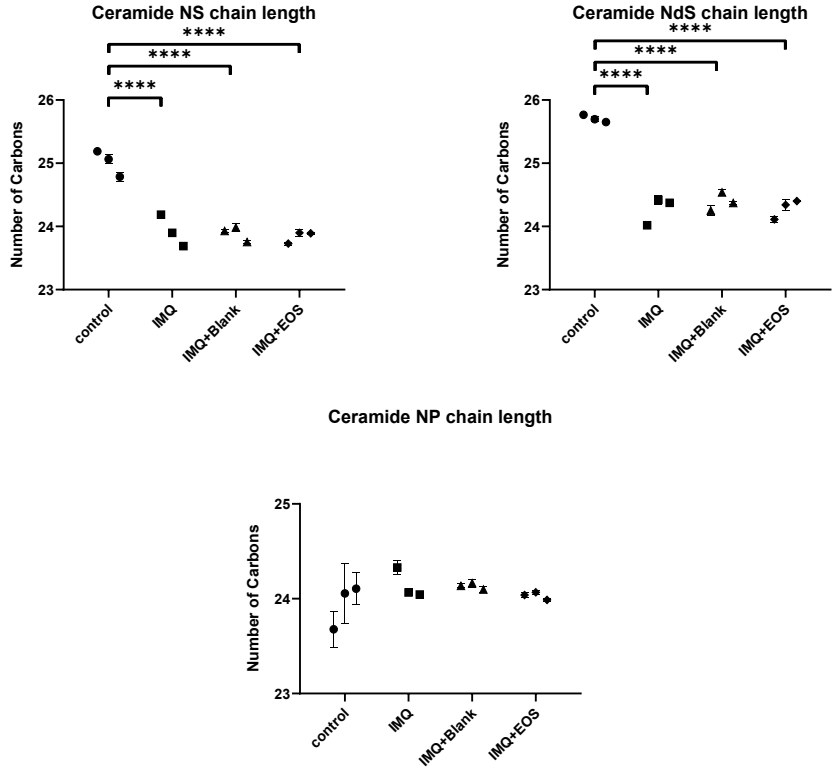

Figure 12. Average acyl chain lengths of non-hydroxylated ceramides. Data are shown as mean (± SEM, n =3). Asterisks: p < 0.0001 (****).

In the present study, as illustrated in **Figure 12**, we observed a decreasing trend in acyl chain lengths for CER NS and CER NdS across all treatment groups compared to the control, which correlates with increased transepidermal water loss and impaired barrier permeability. Despite this trend, no statistically significant differences were found among the treatment

groups. Furthermore, no significant differences were observed among the treatment groups in the case of CER NP.

4.5.3 Profile of Non-hydroxylated ceramides (N)

To better understand the distribution of acyl chain lengths, we calculated the ceramide profile for each ceramide subclass. The ceramide profile was determined by the presence percentage of each acyl chain length within each ceramide subclass across individual mice and subsequently averaged for all mice of each group as mean ± SEM.

Upon examining the ceramide profile as illustrated in **Figure 13**, it becomes evident that there is a pronounced decrease in C26 and an increase in C24 distribution of acyl chains for both ceramides NS and NdS across all treatment groups compared to the control. This observation aligns with the results obtained from analyzing average chain lengths, reinforcing the consistency of this trend.

Interestingly, even though the statistical analysis of average chain lengths did not reveal a significant difference in the case of ceramide NP, a closer inspection of its profile reveals a noticeable increase in C24 and a decrease in C22 and C26 distribution of acyl chains in all treatment groups relative to the control. This suggests that, while the average chain lengths may remain similar to the control, the distribution pattern indicates a preference for the C24 acyl chain for CER NP in the psoriatic lesions in our models.

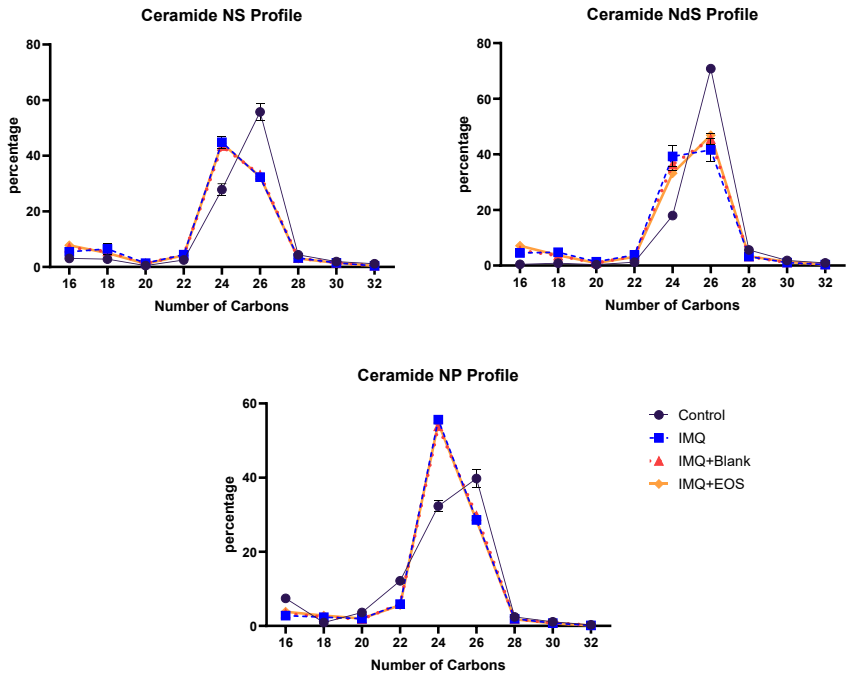

Figure 13. Profile of percentage distribution of fatty acyl chain lengths for non-hydroxylated ceramides. Data are shown as average for all mice of each group as mean (± SEM, n =3).

4.6 Quantification of α-hydroxylated ceramides (A)

Similar to N ceramides, the quantification of α-hydroxylated ceramides was performed by summing all determined chain lengths, which include the C18 sphingoid base along with acyl chain lengths ranging from 16 to 32 carbons.

4.6.1 Total content of α-hydroxylated ceramides (A)

For CER AS, (**Figure 14**) an increasing trend was observed across all treatment groups, with the IMQ+EOS group showing the most pronounced increase. This aligns with findings from previous studies.[90] However, for CER AdS, our results contrasted with those studies, showing a decreasing trend across all treatment groups compared to the control. The IMQ+EOS group exhibited the least pronounced decrease, with a significant difference from both the IMQ and IMQ+Blank groups. Another interesting result in contrast to previous findings similar to what was observed for CER NP, was achieved in the case of CER AP.[45,90] There was a significant increase among all treatment groups compared to the control, with the IMQ+EOS group showing the most pronounced rise.

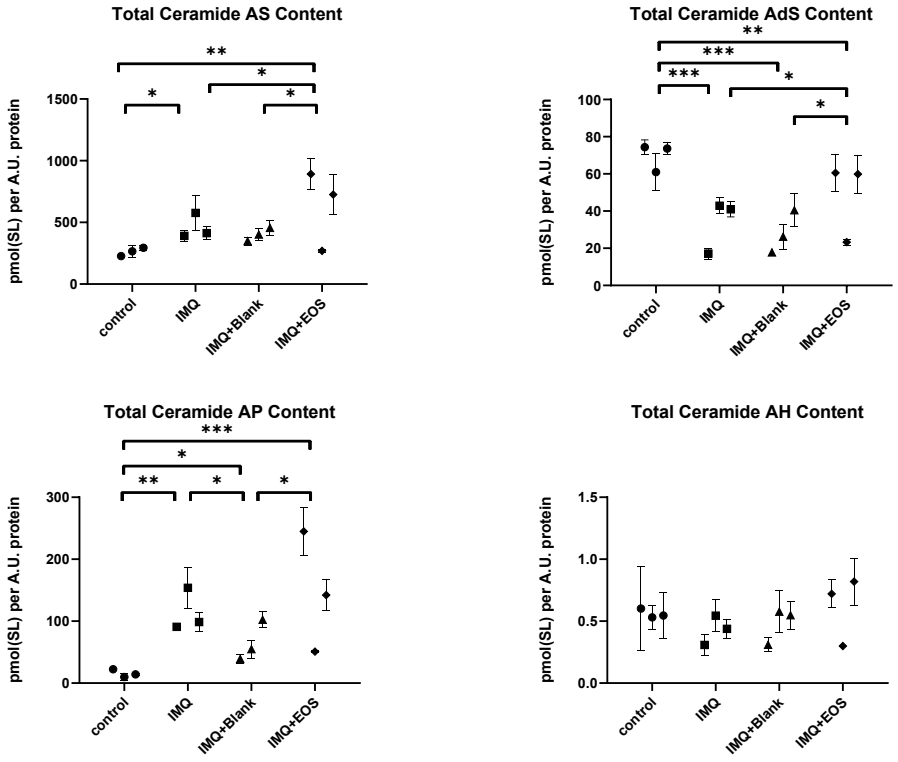

Figure 14. Quantification of α-hydroxylated ceramides. Data are shown as mean (± SEM, n =3). Asterisks: p < 0.05 (*), p < 0.01 (**), p < 0.001 (***)

During ceramide synthesis, the transition from dS ceramides to S and P ceramides occurs through the activity of specific enzymes. DEGS 1 converts dS ceramides, such as CER NdS and CER AdS, into Sph-CERs. Concurrently, DESG 2 transforms these dS ceramides into Phyto-CERs.[39] The observed alterations in ceramide levels may reflect changes in the activity of these enzymes within psoriatic lesions, highlighting the intricate dynamics of ceramide regulation in psoriasis. The observed increase in Phyto-SphCERs correlated with higher TEWL. This connection highlights an intriguing area for future research into how Phyto-CERs might influence skin permeability and their role in psoriatic lesions.

4.6.2 Average acyl chain lengths of α-hydroxylated ceramides (A)

Regarding the acyl chain lengths of α-hydroxy ceramides, we observed a similar trend for CERs AS and AdS, with a decrease in chain length similar to CERs NS and NdS. (**Figure 15**) Notably, for CER AdS, the treatment group with EOS cream exhibited a less pronounced decrease compared to both IMQ and IMQ+Blank groups, suggesting a probable effect of EOS cream in improving acyl chain length for this ceramide subclass.

Interestingly, this trend does not apply to CER AP, where an opposite pattern is observed, showing an increase in all treatment groups compared to the control. However, there was no significant difference among the treatment groups themselves.

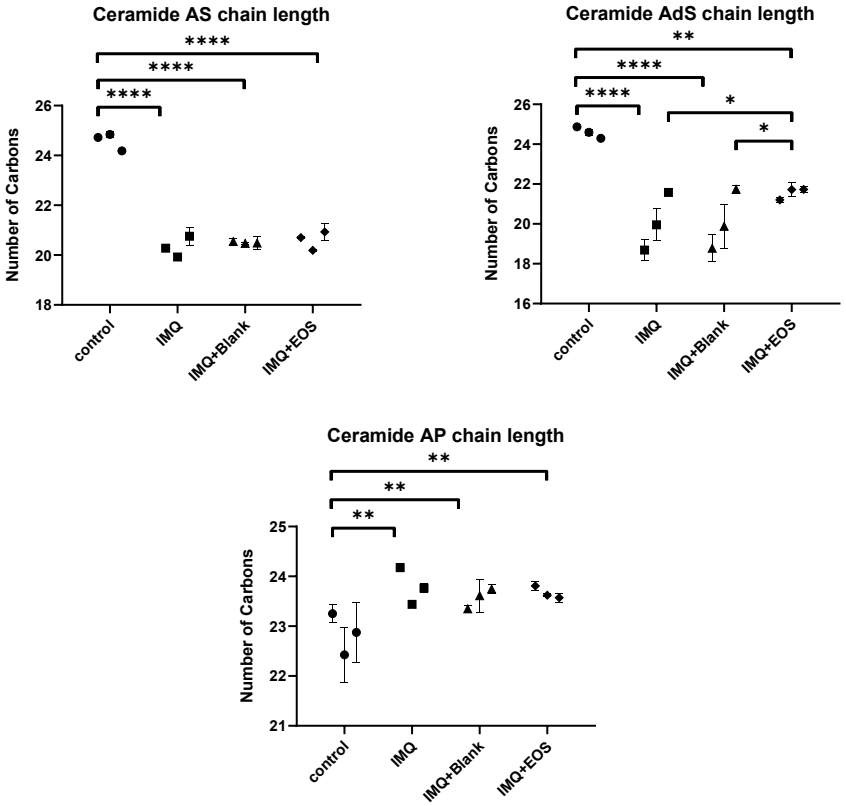

Figure 15. The average acyl chain lengths of α-hydroxylated ceramides. Data are shown as mean (± SEM, n =3). Asterisks: p < 0.05 (*), p < 0.01 (**), p < 0.0001 (****).

4.6.3 Profile of α-hydroxylated ceramides (A)

Analyzing the ceramide profile of α-hydroxy ceramides as depicted in **Figure 16**, reveals significant changes among the treatment groups. Notably, CERs AS and AdS show an increase in C16 ceramides and a decrease in C26 ceramides, with a shift towards shorter chain lengths compared to CERs NS and NdS. This suggests a favorable shift towards shorter chain lengths in psoriatic lesions for CERs AS and AdS. Additionally, for CER AdS, the IMQ+EOS group exhibits a distinct profile from the other treatment groups, indicating a potential beneficial effect of EOS cream in slightly enhancing the CER AdS composition towards that seen in the Control group. For CER AP, a decrease in C16, C22, and C26 was observed, accompanied by a shift specifically toward C24. This pattern, resembling the changes observed in CER NP, underscores a compelling area for further investigation into the impact of CER AP24 on skin permeability, particularly in comparison to CER AS24.

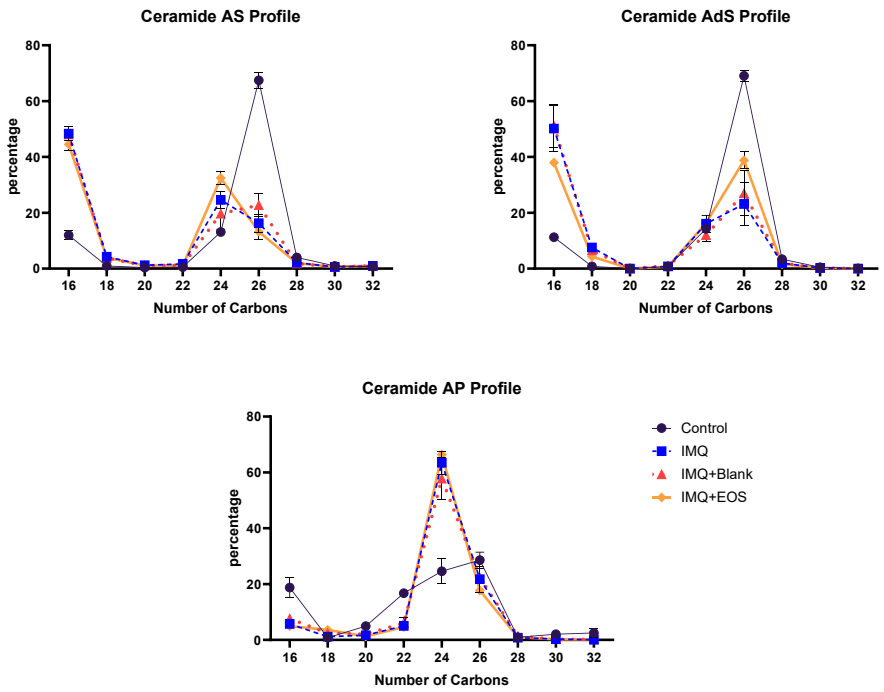

Figure 16. Profile of percentage distribution of fatty acyl chain lengths for α -hydroxylated ceramides. Data are shown as average for all mice of each group as mean (± SEM, n =3).

4.7 Quantification of Esterified ω-hydroxylated ceramides (EO)

Along with other ceramides, ω-esterified ceramides, also known as Acylceramides, were quantified. These Acylceramides are distinguished by their ultra-long ω-hydroxylated chains, ranging from 26 to 36 carbons, esterified with linoleic acid. EO ceramides are unique to the epidermis and have a distinctive structure critical for forming and stabilizing lipid organization in the lipid lamellae.

4.7.1 The total content of Esterified ω-hydroxylated ceramides (EO)

Numerous studies have shown that Acylceramides are essential for forming the skin permeability barrier. Reduced levels of EOS ceramides, a key Acylceramide, have been linked to skin barrier dysfunction. CerS3 is the only ceramide synthase capable of generating specific ULCFAs exceeding 26 carbons, including ω-hydroxy ULCFAs.[94,95]

Here, similar to the analysis of total ceramide content, EOS29 was excluded from the CER EOS analysis to better understand the changes. As illustrated in **Figure 17**, an increase in CER EOS was observed only in the IMQ group, while the IMQ+EOS group also showed an increase, though it was not statistically significant. For CER EOdS, a decreasing trend was noted across all treatment groups compared to the control, but these changes were not statistically significant between the groups themselves. In contrast, CER EOP, like CER NP and CER AP, exhibited

an increasing trend among the treatment groups, with the IMQ+EOS group showing a significantly greater increase than the other groups.

A recent study by Opalka et al. demonstrated that specific Acylceramides, particularly CER EOS, form more stable lamellar structures compared to ceramide EOP, which has less ability to form long periodicity phase (LPP) structures.[96] Our results, consistent with these findings, may underscore the involvement of Phyto-CERs in permeability barrier disruption, which in our study correlated with TEWL.

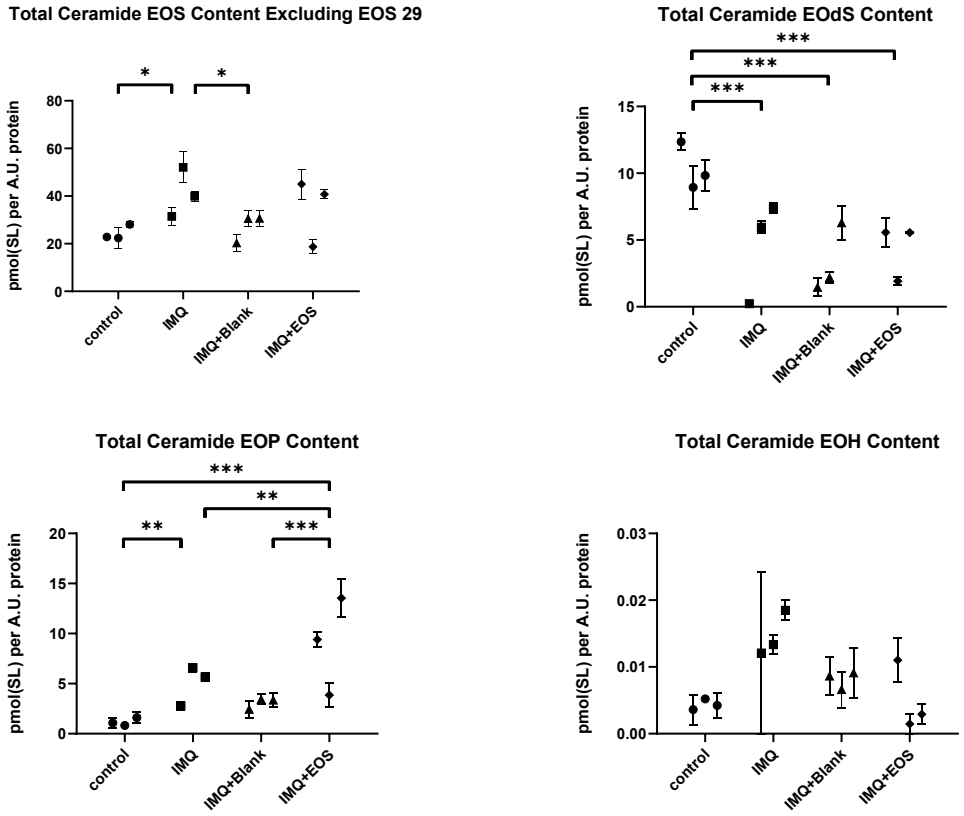

Figure 17. Quantification of ω-esterified ceramides. Data are shown as mean (± SEM, n =3). Asterisks: group p < 0.05 (*), p < 0.01 (**), p < 0.001 (***).

4.7.2 Average acyl chain lengths of ω-esterified ceramides (EO)

Analysis of the acyl chain lengths of EO ceramides as demonstrated in **Figure 18**, revealed a significant decrease in the group treated with EOS cream for both EOS and EOP ceramides. This group showed a statistically significant reduction in acyl chain lengths compared to the control and other treatment groups, highlighting the potential involvement of EOS cream in altering ceramide synthesis and the effect of change in acyl chain lengths. It has been shown that levels of CerS3 and ELOVL4 are downregulated in psoriatic lesions, which may partially

explain the observed decrease in Acylceramides and the associated changes in permeability barrier function.[85]

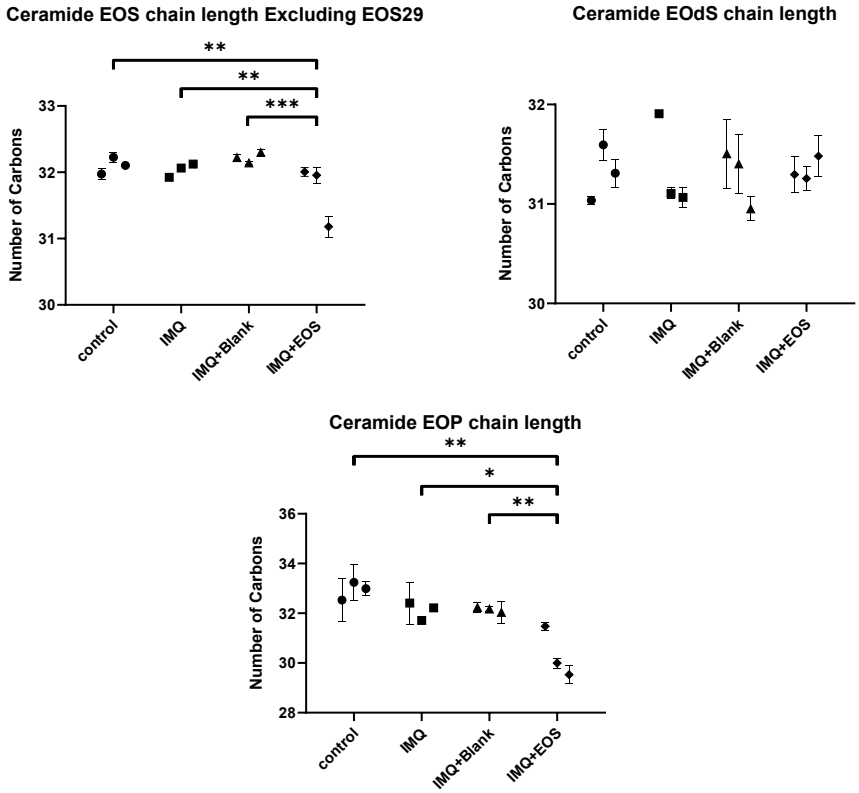

Figure 18. The average acyl chain lengths of ω-esterified ceramides. Data are shown as mean (± SEM, n =3). Asterisks: p < 0.05 (*), p < 0.01 (**), p < 0.001 (***).

4.7.3 Profile of ω-esterified ceramides (EO)

Examining the ceramide profile to better understand changes in chain lengths, as shown in **Figure 19**, reveals that in the EOS cream-treated group, we observed a decrease in C32 and an increase in C28 containing ceramides. For CER EOdS, a similar profile is observed across all groups. For CER EOP, both IMQ and IMQ+Blank groups show a favorable shift toward C32 and a decrease in C34 and C36. For the IMQ+EOS group, we observed similar changes in C34 and C36 acyl chains. In contrast to the other treatment groups, this group showed a decrease in C32 and a significant increase in C28 acyl chains, highlighting a shift towards shorter acyl chain lengths. As demonstrated in previous studies, decreases in acyl chain lengths have been linked to increased permeability,[93] a trend observed across all our treatment groups, with the effect being most pronounced in the IMQ+EOS group.

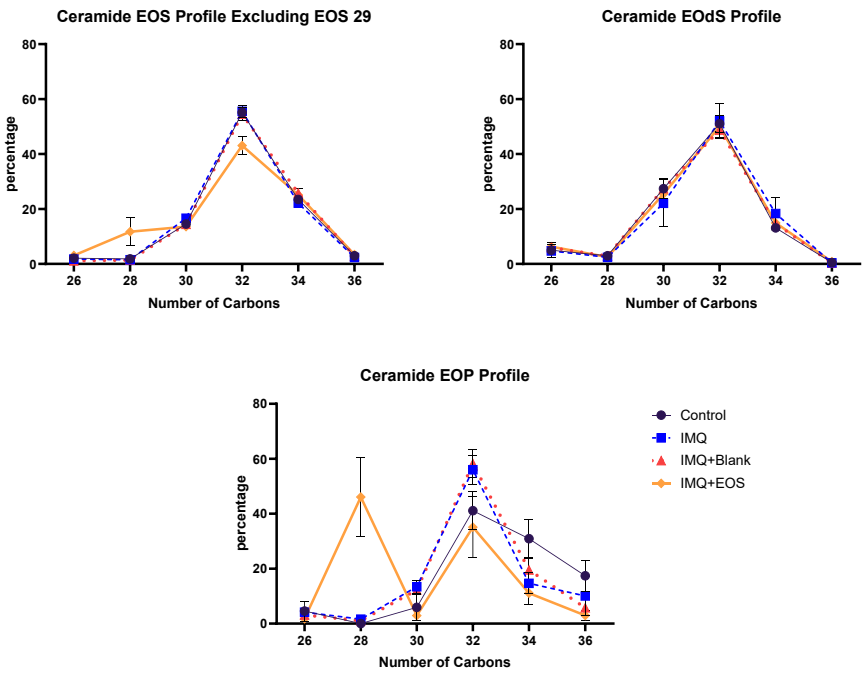

Figure 19. The profile of percentage distribution of fatty acyl chain lengths for ω-esterified ceramides. Data are shown as average for all mice of each group as mean (± SEM, n =3).

.

To confirm the successful delivery of CER EOS29 to the SC, we included it in the ceramide profile of EOS, as illustrated in **Figure 20**. The percentage distribution of acyl chains clearly shows a dominant presence of C29, thereby confirming the effective delivery of EOS29.

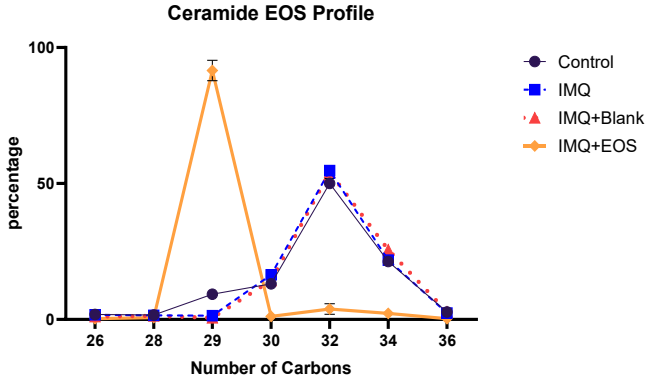

Figure 20. The profile of percentage distribution of fatty acyl chain lengths for ω-esterified ceramides including EOS29. Data are shown as average for all mice of each group as mean (± SEM, n =3).

4.8 Quantification of ω-hydroxylated ceramides (O)

ω-Hydroxylated ceramides share similarities with Acylceramides in possessing ultra-long acyl chains, generally ranging from 26 to 36 carbon atoms. However, a key distinction is that ω-hydroxylated ceramides are not subjected to further esterification, unlike Acylceramides.

4.8.1 The total content of ω-hydroxylated ceramides (O)

During the analysis, ω-hydroxy ceramides with ultra-long chains ranging from 26 to 36 carbons were quantified. (**Figure 21**) Regarding these ω-hydroxy ceramides, CER OS showed an increasing trend in all treatment groups compared to the control, with the IMQ+EOS group exhibiting a statistically significant increase relative to the other treatment groups. For CER OdS, only the IMQ+EOS group displayed statistical significance when compared to the other groups, including the control. In the case of CER OP, a similar increasing trend was observed as with previous Phyto-CER subclasses; however, no statistically significant differences were noted between the treatment groups. ω-Hydroxy ceramides are usually found in small quantities in healthy human SC because they serve as precursors to Acylceramides and are primarily converted into Acylceramides by the enzyme PNPLA1, which aids in their ω-esterification.[97] The pronounced increase in CER OP further underscores the importance of Phyto-CERs and their role in skin barrier disruption, consistent with observations in previous Phyto-Sph containing subclasses.

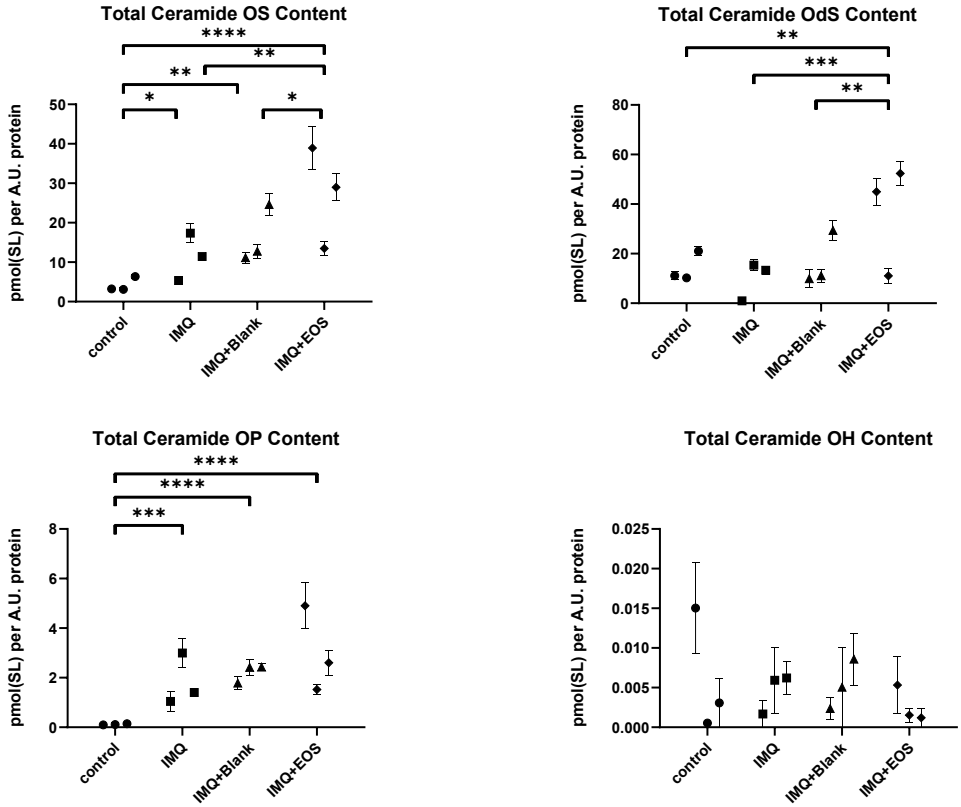

Figure 21. Quantification of ω-hydroxy ceramides. Data are shown as mean (± SEM, n =3).Asterisks: p < 0.05 (*), p < 0.01 (**), p < 0.001 (***),p < 0.0001 (****).

4.8.2 Average acyl chain lengths of ω-hydroxylated ceramides (O)

Examining the acyl chain lengths of OS ceramides represented in **Figure 22**, a decreasing trend was observed across all treatment groups and the control. However, the extent of this decrease varied among the treatment groups. The IMQ+EOS group exhibited the least decrease, followed by the IMQ+Blank group, and then the IMQ group, which showed the most pronounced decrease. For CER OdS, a decrease was observed between the IMQ+EOS group and both the control and IMQ+Blank groups. Conversely, for CER OP no change in average acyl chain length was observed.

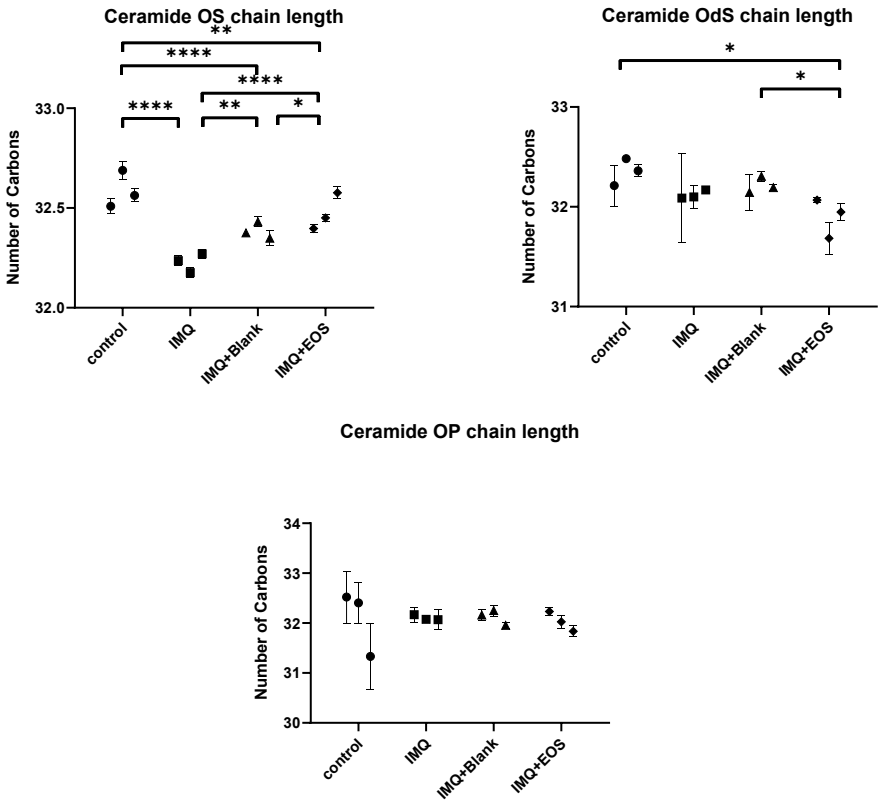

Figure 22. The average acyl chain lengths of ω-hydroxy ceramides. Data are shown as mean (± SEM, n =3). Asterisks: p < 0.05 (*), p < 0.01 (**), p < 0.0001 (****).

4.8.3 Profile of ω-hydroxylated ceramides (O)

Examining the ω-hydroxy ceramide profiles shown in **Figure 23**, we found that although changes in acyl chain lengths were statistically significant, their overall magnitude was relatively minor. This is supported by the ceramide distribution profiles, which were similar among treatment groups compared to the control for CER OS, showing only a slight decrease in C34 and a minor increase in C32. For CER OdS, the IMQ+EOS group displayed notable changes, specifically a decrease in C34 and an increase in C28.

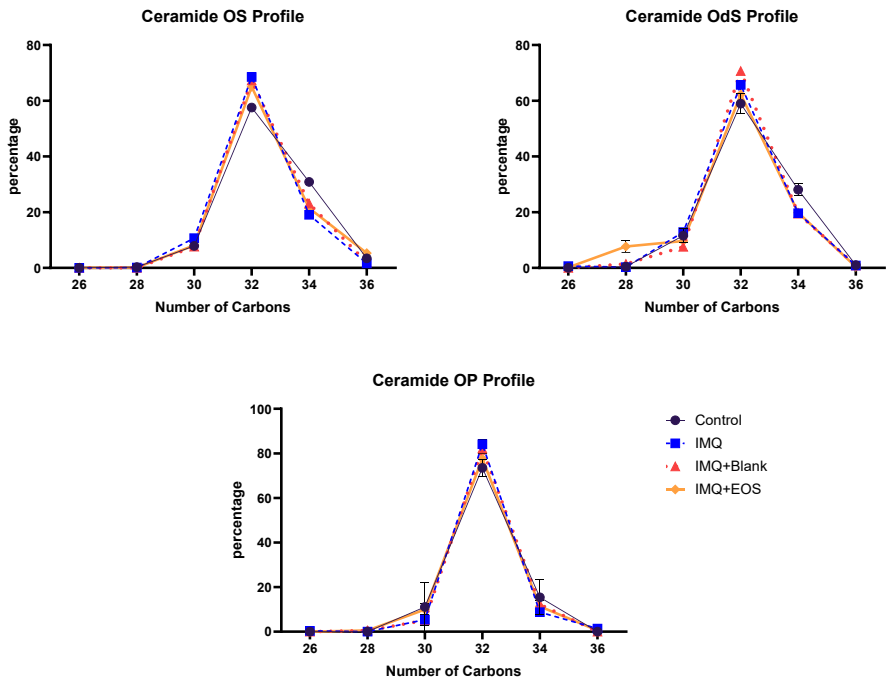

Figure 23. The profile of percentage distribution of fatty acyl chain lengths for ω-hydroxy ceramides. Data are shown as average for all mice of each group as mean (± SEM, n =3).

4.9 Percentage representation of individual subclasses of ceramides

In this section, we employed an alternative approach to elucidate changes in CER levels by analyzing the results in terms of their percentages. (**Figure 24**) Unlike the previous sections that presented absolute values, we now present relative values, specifically the ratio of individual subclasses to the total amount of ceramides in each group. As observed in previous studies, not only the absolute levels of CERs but also the percentage presence of each CER subclass contributes to the integrity and permeability of the SC in PSO.[40]

As observed in the previous graphs concerning Phyto-CERs, we observed an increasing trend for CER NP and a more modest increase in the case of CER AP among our treatment groups compared to the control. Notably, there is a significant decrease in ceramides derived from sphingosine (CER AS) and dihydrosphingosine (CER AdS), which suggests a preferential hydroxylation of dihydroceramides at position 4, leading to an increase in Phyto-Sph derived ceramides. This change occurs at the expense of competitive desaturation processes that normally produce Sph-derived ceramides. The increase in CER NS, however, is observable only in low percentage change. In a recent study, the authors proposed that a higher CERs NP/NS ratio indicates healthy skin conditions, while a lower ratio is associated with poor or undifferentiated skin conditions;[98] however, our results, which reveal an opposite trend in the treatment groups, are in contrast with their findings.

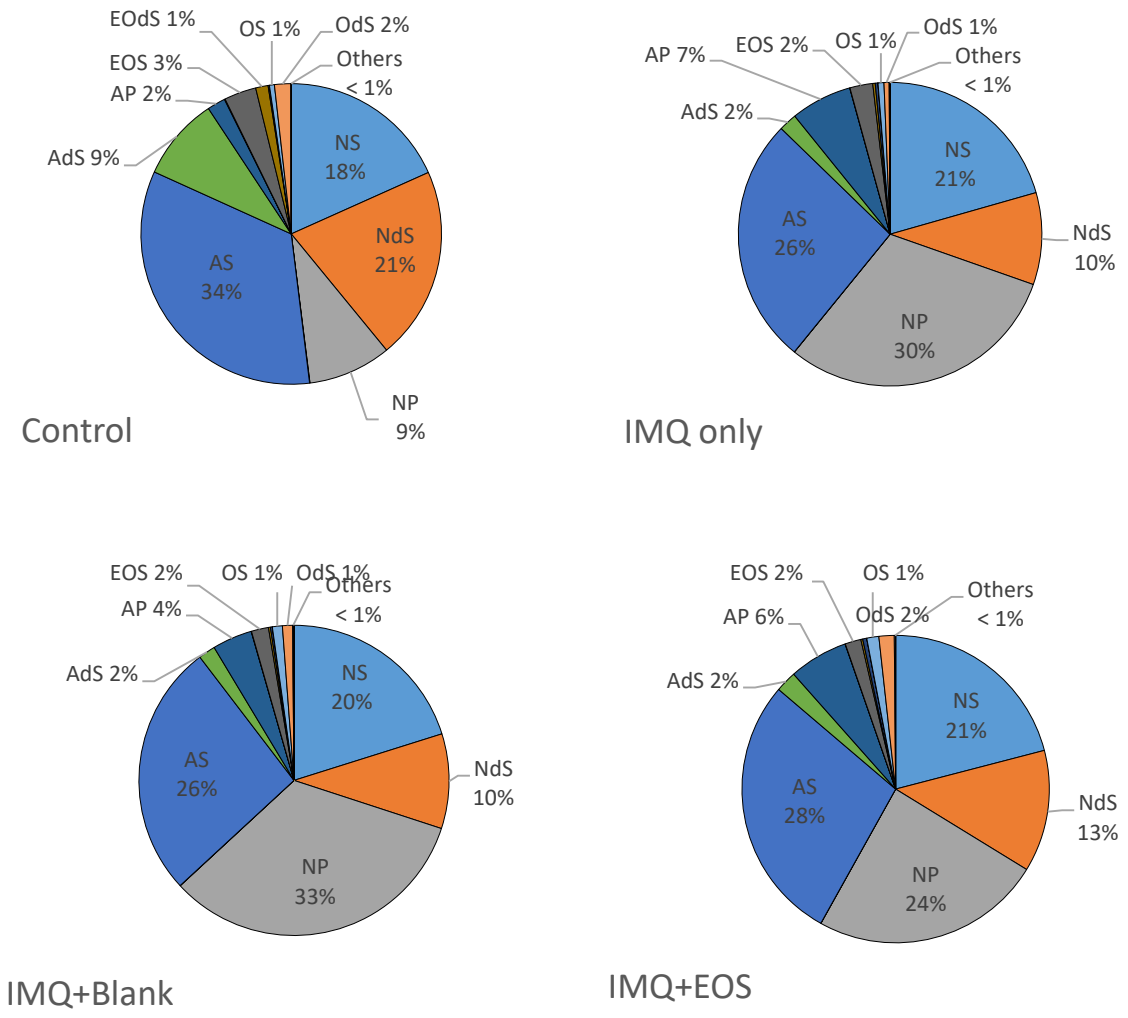

Figure 24. Percentage representation of all measured ceramides; The values shown in the graphs represent the mean values obtained by averaging the results of each ceramide subclass within each group. These values reflect the average of all 3 mice in each respective group (with all data points from previous analyses averaged for this chart).

4.10 The ratio between very-long and ultra-long ceramides

By determining this ratio, we aimed to assess whether there are any changes in the synthesis of ultra-long chain ceramides in a mouse model of induced psoriasis. These ceramides share some aspects of their biosynthesis with other ceramides but differ in the final stages of their synthesis. As displayed in **Figure 25**, we observed a statistically significant increase in the ratio of VLC-CERs to ULC-CERs for the IMQ and IMQ+Blank groups compared to the control. Interestingly, the IMQ+EOS group did not exhibit a significant increase and showed a ratio more similar to the control than the other treatment groups.

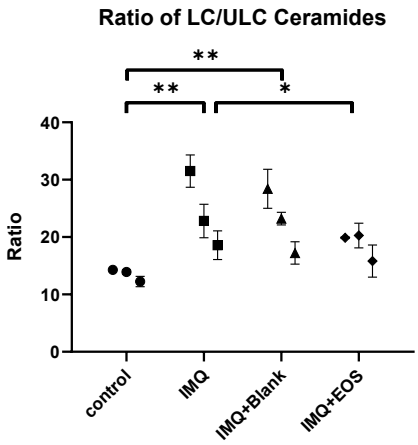

Figure 25. The ratio between the content of very long and ultra-long chain ceramides (dimensionless quantity). Data are presented as mean (± SEM, n =3).Asterisks: p < 0.05 (*), p < 0.01 (**).

Many studies have indicated that a decrease in ULC-CERs is characteristic of PSO pathogenesis, which was suggested it's a result of the downregulation of CerS3 and ELOVL4.[9,85] Reduced amounts of Acylceramides or their complete absence in model lipid membranes, which are characteristic of skin diseases such as AD, lead to decreased lipid ordering, an absent or reduced long periodicity lamellar phase, and increased permeability compared to physiologically composed membranes.[96] We observe a similar trend with an increase in short-chain ceramides and a correlation with TEWL. Although the content of Acylceramides is slightly reduced at the expense of other ceramides, contributing to increased TEWL values, the change in Acylceramide levels is not the sole factor. For instance, increased TEWL values were also observed in the IMQ+EOS group, where a decrease in Acylceramide levels was noted to a lesser extent, yet TEWL exhibited a similar profile to that of other treatment groups.

5. CONCLUSION

The primary objective of this study was to evaluate the effect of 0.5% ceramide EOS29 cream on a mouse model of induced psoriasis. This was achieved by quantifying ceramides in the stratum corneum and measuring transepidermal water loss (TEWL) in the subjects. Additionally, the total protein and ceramide content were determined in the collected samples, with protein content used to normalize ceramide levels to account for sampling variability. Lipid analysis provided insights into the distribution of ceramide subclasses and their detailed evaluation based on average acyl chain lengths. Specifically, the ratio between long-chain ceramides (N-ceramides and A-ceramides) and ultra-long-chain ceramides (O-ceramides and EO-ceramides) was assessed.

TEWL was measured daily for four days before and at hourly intervals for three hours after skin sampling, revealing higher levels in the group treated with EOS cream compared to the IMQ and IMQ+Blank groups, both before and after sampling. After sampling TEWL levels followed the order: IMQ+EOS > IMQ+Blank > IMQ, with all treated groups exhibiting higher TEWL compared to healthy controls. These findings suggest a potential defect in the skin barrier function in the treated groups and a decreased ability of the skin to regenerate after damage compared to the control.

After normalizing the total ceramide content to protein levels, the treatment groups exhibited elevated ceramide levels compared to the control group, with the IMQ+EOS group showing the highest increase. When examining ceramide levels based on the sphingoid base structure, there was a general increase in ceramides derived from sphingosine (S) and phytosphingosine (P). Additionally, ceramides containing dihydrosphingosine (dS) were elevated only in the IMQ+EOS group compared to the others.

Analyzing the acyl chains of ceramides, the most significant increase was found in non-hydroxy (N) ceramides, with NP and NS ceramides showing the greatest elevation. Similarly, α-hydroxy ceramides (A), particularly AP ceramides, also showed substantial increases. Changes in ω-esterified ceramides (EO) varied between groups, but EOP ceramides demonstrated the most pronounced increase. For ω-hydroxy ceramides (O), OP ceramides exhibited the highest increase. These findings highlighted the possible involvement of Phytosphingosine ceramides in skin barrier dysfunction.

The average acyl chain lengths of ceramides showed a decreasing trend for NS, NdS, AS, AdS, and OS ceramides, whereas an increase was observed for AP ceramides. For ω-esterified (EO) ceramides, a decrease in acyl chain length was noted exclusively in the IMQ+EOS group

compared to the other groups. These findings showed the relation of decreased acyl chain lengths with alteration of skin barrier function.

Analyzing the ratio of long-chain to ultra-long-chain ceramides revealed an increase for both the IMQ and IMQ+Blank groups. However, the IMQ+EOS group did not exhibit any significant increase in this ratio.

The main goal was to assess the effect of EOS cream on induced psoriasis. While a positive effect was not fully achieved, and no significant difference in TEWL was observed, the ratio of long-chain to ultra-long-chain ceramides was improved. Our findings underscore the complex effects of exogenous ceramide EOS on skin barrier properties and their potential impacts on skin health. These results highlight the intricate nature of ceramide interactions within the skin and suggest that while 0.5% ceramide EOS cream may not significantly affect TEWL, it does influence the ceramide profile, particularly the ratio of long-chain to ultra-long-chain ceramides.

The findings of this study indicate that a comprehensive understanding of the effects of exogenous EOS ceramides and their implications for treating skin conditions like psoriasis requires careful experimentation with varying concentrations of ceramide EOS cream. Future research should explore these different concentrations to fully elucidate their therapeutic potential in this context.

6. REFERENCES

1. Matwiejuk M, Mysliwiec H, Chabowski A, Flisiak I. The role of sphingolipids in the pathogenesis of psoriasis. Metabolites. 2022;12(12):1171.
2. Uchida Y, Park K. Ceramides in skin health and disease: An update. Am J Clin Dermatol. 2021;22(6):853-66.
3. Shin KO, Mihara H, Ishida K, Uchida Y, Park K. Exogenous ceramide serves as a precursor to endogenous ceramide synthesis and as a modulator of keratinocyte differentiation. Cells. 2022;11(11):1742.
4. Berkers T, Visscher D, Gooris GS, Bouwstra JA. Topically applied ceramides interact with the stratum corneum lipid matrix in compromised ex vivo skin. Pharm Res. 2018;35:48.
5. Yousef H, Alhajj M, Sharma S. Anatomy, skin (integument), epidermis. In: StatPearls [Internet]. Treasure Island (FL): StatPearls Publishing; 2024. PMID: 29262154.
6. Knox S, O'Boyle NM. Skin lipids in health and disease: A review. Chem Phys Lipids. 2021;236:105055.
7. Zwara A, Wertheim-Tysarowska K, Mika A. Alterations of ultra long-chain fatty acids in hereditary skin diseases-review article. Front Med (Lausanne). 2021;8:73085520.
8. Brown TM, Krishnamurthy K. Histology, dermis. In: StatPearls [Internet]. Treasure Island (FL): StatPearls Publishing; 2024. PMID: 30570967.
9. McGrath JA, Eady RA, Pope FM. Anatomy and organization of human skin. In: Rook's textbook of dermatology. 2004. p. 45-128.
10. Kolarsick PA, Kolarsick MA, Goodwin C. Anatomy and physiology of the skin. J Dermatol Nurses Assoc. 2011;3(4):203-13.
11. Murphrey MB, Miao JH, Zito PM. Histology, stratum corneum. In: StatPearls [Internet]. Treasure Island (FL): Stat Pearls Publishing; 2024.
12. van Smeden J, Janssens M, Gooris GS, Bouwstra JA. The important role of stratum corneum lipids for the cutaneous barrier function. BiochimBiophysActa. 2014;1841(3):295-313.
13. Wickett RR, Visscher MO. Structure and function of the epidermal barrier. Am J Infect Control. 2006;34(10 Suppl)

14. Elias PM. Epidermal lipids, barrier function, and desquamation. J Invest Dermatol. 1983;80(1 Suppl):44s-9s.
15. Évora AS, Adams MJ, Johnson SA, Zhang Z. Corneocytes: Relationship between structural and biomechanical properties. Skin Pharmacol Physiol. 2021;34(3):146-62.
16. Madison KC. Barrier function of the skin: "la raison d'être" of the epidermis. J Invest Dermatol. 2003;121(2):231-41.
17. Takeichi T, Hirabayashi T, Miyasaka Y, Kawamoto A, Okuno Y, Taguchi S, et al. SDR9C7 catalyzes critical dehydrogenation of acylceramides for skin barrier formation. J Clin Invest. 2020;130(2):890-903.
18. Iwai I, Han H, den Hollander L, Svensson S, Ofverstedt LG, Anwar J, et al. The human skin barrier is organized as stacked bilayers of fully extended ceramides with cholesterol molecules associated with the ceramide sphingoid moiety. J Invest Dermatol. 2012;132(9):2215-25.
19. Ishida-Yamamoto A, Igawa S. The biology and regulation of corneodesmosomes. Cell Tissue Res. 2015;360(3):477-82.
20. Cha HJ, He C, Zhao H, Dong Y, An IS, An S. Intercellular and intracellular functions of ceramides and their metabolites in skin (Review). Int J Mol Med. 2016;38(1):16-22.
21. Jiao Q, Yue L, Zhi L, Qi Y, Yang J, Zhou C, et al. Studies on stratum corneum metabolism: function, molecular mechanism and influencing factors. J CosmetDermatol. 2022;21(8):3256-64.
22. Kezic S, Jakasa I. Filaggrin and skin barrier function. CurrProblDermatol. 2016;49:1-7.
23. Wertz PW. Lipid metabolic events underlying the formation of the corneocyte lipid envelope. Skin Pharmacol Physiol. 2021;34(1):38-50.
24. van Smeden J, Bouwstra JA. Stratum corneum lipids: Their role for the skin barrier function in healthy subjects and atopic dermatitis patients. CurrProblDermatol. 2016;49:8-26.
25. Feingold KR. Thematic review series: skin lipids. The role of epidermal lipids in cutaneous permeability barrier homeostasis. J Lipid Res. 2007;48(12):2531-46.
26. Mijaljica D, Townley JP, Spada F, Harrison IP. The heterogeneity and complexity of skin surface lipids in human skin health and disease. Prog Lipid Res. 2024;93:101264.
27. Vávrová K, Kováčik A, Opálka L. Ceramides in the skin barrier. Eur Pharm J. 2017;64(2):28-35.

28. Rabionet M, Gorgas K, Sandhoff R. Ceramide synthesis in the epidermis. BiochimBiophysActa. 2014;1841(3):422-34.
29. Coderch L, López O, de la Maza A, Parra JL. Ceramides and skin function. Am J ClinDermatol. 2003;4(2):107-29.
30. Wertz P. Epidermal lamellar granules. Skin Pharmacol Physiol. 2018;31(5):262-8.
31. Madison KC, Swartzendruber DC, Wertz PW, Downing DT. Presence of intact intercellular lipid lamellae in the upper layers of the stratum corneum. J Invest Dermatol. 1987;88(6):714-8.
32. Bouwstra JA, Nădăban A, Bras W, McCabe C, Bunge A, Gooris GS. The skin barrier: An extraordinary interface with an exceptional lipid organization. Prog Lipid Res. 2023;92:101252.
33. Elias PM, Williams ML, Choi EH, Feingold KR. Role of cholesterol sulfate in epidermal structure and function: lessons from X-linked ichthyosis. BiochimBiophysActa. 2014;1841(3):353-61.
34. Kihara A. Synthesis and degradation pathways, functions, and pathology of ceramides and epidermal acylceramides. Prog Lipid Res. 2016;63:50-69.
35. Gray GM, Yardley HJ. Lipid compositions of cells isolated from pig, human, and rat epidermis. J Lipid Res. 1975;16(6):434-40.
36. Gray GM, White RJ. Glycosphingolipids and ceramides in human and pig epidermis. J Invest Dermatol. 1978;70(6):336-41.
37. VietriRudan M, Watt FM. Mammalian epidermis: A compendium of lipid functionality. Front Physiol. 2022;12:804824.
38. Mizutani Y, Mitsutake S, Tsuji K, Kihara A, Igarashi Y. Ceramide biosynthesis in keratinocyte and its role in skin function. Biochimie. 2009;91(6):784-90.
39. Bouwstra JA, Dubbelaar FE, Gooris GS, Ponec M. The lipid organisation in the skin barrier. ActaDermVenereolSuppl (Stockh). 2000;208:23-30.
40. Choi MJ, Maibach HI. Role of ceramides in barrier function of healthy and diseased skin. Am J ClinDermatol. 2005;6(4):215-23.
41. t'Kindt R, Jorge L, Dumont E, Couturon P, David F, Sandra P, et al. Profiling and characterizing skin ceramides using reversed-phase liquid chromatography-quadrupole time-of-flight mass spectrometry. Anal Chem. 2012;84(1):403-11.
42. Suzuki M, Ohno Y, Kihara A. Whole picture of human stratum corneum ceramides, including the chain-length diversity of long-chain bases. J Lipid Res. 2022;63(6):100217.

43. Kawana M, Miyamoto M, Ohno Y, Kihara A. Comparative profiling and comprehensive quantification of stratum corneum ceramides in humans and mice by LC/MS/MS. J Lipid Res. 2020;61(6):884–95.
44. Kováčik A, Roh J, Vávrová K. The chemistry and biology of 6-hydroxyceramide, the youngest member of the human sphingolipid family. Chembiochem. 2014 Jul 21;15(11):1555-62.
45. Motta S, Monti M, Sesana S, Caputo R, Carelli S, Ghidoni R. Ceramide composition of the psoriatic scale. BiochimBiophysActa. 1993;1182(2):147–51.
46. Robson KJ, Stewart ME, Michelsen S, Lazo ND, Downing DT. 6-Hydroxy-4-sphingenine in human epidermal ceramides. J Lipid Res. 1994 Nov;35(11):2060-8.
47. Ge F, Sun K, Hu Z, Dong X. Role of Omega-Hydroxy Ceramides in Epidermis: Biosynthesis, Barrier Integrity and Analyzing Method. Int J Mol Sci. 2023 Mar 6;24(5):5035.
48. Breiden B, Sandhoff K. The role of sphingolipid metabolism in cutaneous permeability barrier formation. BiochimBiophysActa. 2014 Mar;1841(3):441-52.
49. Jia ZX, Zhang JL, Shen CP, Ma L. Profile and quantification of human stratum corneum ceramides by normal-phase liquid chromatography coupled with dynamic multiple reaction monitoring of mass spectrometry: development of targeted lipidomic method and application to human stratum corneum of different age groups. Anal Bioanal Chem. 2016 Sep;408(24):6623-36.
50. Masukawa Y, Narita H, Shimizu E, Kondo N, Sugai Y, Oba T, et al. Characterization of overall ceramide species in human stratum corneum. J Lipid Res. 2008 Jul;49(7):1466-76.
51. Hannun YA, Obeid LM. Sphingolipids and their metabolism in physiology and disease. Nat Rev Mol Cell Biol. 2018 Mar;19(3):175-191.
52. Bocheńska K, Gabig-Cimińska M. Unbalanced Sphingolipid Metabolism and Its Implications for the Pathogenesis of Psoriasis. Molecules. 2020 Mar 3;25(5):1130.
53. Michel C, van Echten-Deckert G, Rother J, Sandhoff K, Wang E, Merrill AH Jr. Characterization of ceramide synthesis. A dihydroceramide desaturase introduces the 4,5-trans-double bond of sphingosine at the level of dihydroceramide. J Biol Chem. 1997 Sep 5;272(36):22432-7.
54. Jojima K, Edagawa M, Sawai M, Ohno Y, Kihara A. Biosynthesis of the anti-lipid-microdomainsphingoid base 4,14-sphingadiene by the ceramide desaturase FADS3. FASEB J. 2020 Feb;34(2):3318-3335.

55. Zeng F, Qin W, Huang F, Chang P. PNPLA1-Mediated Acylceramide Biosynthesis and Autosomal Recessive Congenital Ichthyosis. Metabolites. 2022 Jul 26;12(8):685.
56. Akiyama M. Corneocyte lipid envelope (CLE), the key structure for skin barrier function and ichthyosis pathogenesis. J Dermatol Sci. 2017 Oct;88(1):3-9.
57. Krieg P, Rosenberger S, de Juanes S, Latzko S, Hou J, Dick A, et al. Aloxe3 knockout mice reveal a function of epidermal lipoxygenase-3 as hepoxilin synthase and its pivotal role in barrier formation. J Invest Dermatol. 2013 Jan;133(1):172-80.
58. Meguro S, Arai Y, Masukawa Y, Uie K, Tokimitsu I. Relationship between covalently bound ceramides and transepidermal water loss (TEWL). Arch Dermatol Res. 2000 Sep;292(9):463-8.
59. Wertz PW, Downing DT. Ceramides of pig epidermis: structure determination. J Lipid Res. 1983 Jun;24(6):759-65.
60. Ponec M, Weerheim A, Lankhorst P, Wertz P. New acylceramide in native and reconstructed epidermis. J Invest Dermatol. 2003;120(4):581–8.
61. Selvam R, Radin NS. Quantitation of lipids by charring on thin-layer plates and scintillation quenching: application to ceramide determination. Anal Biochem. 1981 Apr;112(2):338-45.
62. Bleck O, Abeck D, Ring J, Hoppe U, Vietzke JP, Wolber R, et al. Two ceramide subfractions detectable in Cer(AS) position by HPTLC in skin surface lipids of non-lesional skin of atopic eczema. J Invest Dermatol. 1999 Dec;113(6):894-900.
63. Fuchs B, Süss R, Teuber K, Eibisch M, Schiller J. Lipid analysis by thin-layer chromatography--a review of the current state. J Chromatogr A. 2011 May 13;1218(19):2754-74.
64. Masukawa Y, Narita H, Sato H, Naoe A, Kondo N, Sugai Y, et al. Comprehensive quantification of ceramide species in human stratum corneum. J Lipid Res. 2009 Aug;50(8):1708-19.
65. van Smeden J, Boiten WA, Hankemeier T, Rissmann R, Bouwstra JA, Vreeken RJ. Combined LC/MS-platform for analysis of all major stratum corneum lipids, and the profiling of skin substitutes. BiochimBiophysActa. 2014 Jan;1841(1):70-9.
66. Farwanah H, Nuhn P, Neubert R, Raith K. Normal-phase liquid chromatographic separation of stratum corneum ceramides with detection by evaporative light scattering and atmospheric pressure chemical ionization mass spectrometry. Anal ChimActa. 2003;492(1):233-9.

67. Norlén L, Nicander I, Lundsjö A, Cronholm T, Forslind B. A new HPLC-based method for the quantitative analysis of inner stratum corneum lipids with special reference to the free fatty acid fraction. Arch Dermatol Res. 1998 Sep;290(9):508-16.
68. Farwanah H, Wohlrab J, Neubert RH, Raith K. Profiling of human stratum corneum ceramides by means of normal phase LC/APCI-MS. Anal Bioanal Chem. 2005 Oct;383(4):632-7.
69. Vietzke JP, Brandt O, Abeck D, Rapp C, Strassner M, Schreiner V, et al. Comparative investigation of human stratum corneum ceramides. Lipids. 2001 Mar;36(3):299-304.
70. Yano M, Kishida E, Muneyuki Y, Masuzawa Y. Quantitative analysis of ceramide molecular species by high performance liquid chromatography. J Lipid Res. 1998 Oct;39(10):2091-8.
71. Houjou T, Yamatani K, Imagawa M, Shimizu T, Taguchi R. A shotgun tandem mass spectrometric analysis of phospholipids with normal-phase and/or reverse-phase liquid chromatography/electrospray ionization mass spectrometry. Rapid Commun Mass Spectrom. 2005;19(5):654-66.
72. Li Q, Fang H, Dang E, Wang G. The role of ceramides in skin homeostasis and inflammatory skin diseases. J Dermatol Sci. 2020 Jan;97(1):2-8.
73. Rendon A, Schäkel K. Psoriasis Pathogenesis and Treatment. Int J Mol Sci. 2019 Mar 23;20(6):1475.
74. Kircik L, Alexis AF, Andriessen A, Blattner C, Glick BP, Lynde CW, et al. Psoriasis and Skin Barrier Dysfunction: The Role of Gentle Cleansers and Moisturizers in Treating Psoriasis. J Drugs Dermatol. 2023 Aug 1;22(8):773-778.
75. Motta S, Monti M, Sesana S, Mellesi L, Ghidoni R, Caputo R. Abnormality of water barrier function in psoriasis: Role of ceramide fractions. Arch Dermatol. 1994 Apr;130(4):452-6.
76. Motta S, Sesana S, Monti M, Giuliani A, Caputo R. Interlamellar lipid differences between normal and psoriatic stratum corneum. ActaDermVenereolSuppl (Stockh). 1994;186:131-2.
77. Lew BL, Cho Y, Kim J, Sim WY, Kim NI. Ceramides and cell signaling molecules in psoriatic epidermis: Reduced levels of ceramides, PKC-alpha, and JNK. J Korean Med Sci. 2006 Feb;21(1):95-9.
78. Cho Y, Lew BL, Seong K, Kim NI. An inverse relationship between ceramide synthesis and clinical severity in patients with psoriasis. J Korean Med Sci. 2004 Dec;19(6):859-63.

79. Ghadially R, Reed JT, Elias PM. Stratum corneum structure and function correlates with phenotype in psoriasis. J Invest Dermatol. 1996 Oct;107(4):558-64.
80. Farwanah H, Raith K, Neubert RH, Wohlrab J. Ceramide profiles of the uninvolved skin in atopic dermatitis and psoriasis are comparable to those of healthy skin. Arch Dermatol Res. 2005 May;296(11):514-21.
81. Alessandrini F, Stachowitz S, Ring J, Behrendt H. The level of prosaposin is decreased in the skin of patients with psoriasis vulgaris. J Invest Dermatol. 2001 Mar;116(3):394-400.
82. Alessandrini F, Pfister S, Kremmer E, Gerber JK, Ring J, Behrendt H. Alterations of glucosylceramide-beta-glucosidase levels in the skin of patients with psoriasis vulgaris. J Invest Dermatol. 2004 Dec;123(6):1030-6.
83. Hong KK, Cho HR, Ju WC, Cho Y, Kim NI. A study on altered expression of serine palmitoyltransferase and ceramidase in psoriatic skin lesions. J Korean Med Sci. 2007 Oct;22(5):862-7.
84. Borodzicz S, Rudnicka L, Mirowska-Guzel D, Cudnoch-Jedrzejewska A. The role of epidermal sphingolipids in dermatologic diseases. Lipids Health Dis. 2016 Jan 19;15:13.
85. Tawada C, Kanoh H, Nakamura M, Mizutani Y, Fujisawa T, Banno Y, Seishima M. Interferon-γ decreases ceramides with long-chain fatty acids: Possible involvement in atopic dermatitis and psoriasis. J Invest Dermatol. 2014 Mar;134(3):712-718.
86. Moon SH, Kim JY, Song EH, Shin MK, Cho YH, Kim NI. Altered levels of sphingosine and sphinganine in psoriatic epidermis. Ann Dermatol. 2013 Aug;25(3):321-6.
87. Moskot M, Bocheńska K, Jakóbkiewicz-Banecka J, Banecki B, Gabig-Cimińska M. Abnormal sphingolipid world in inflammation specific for lysosomal storage diseases and skin disorders. Int J Mol Sci. 2018 Jan 15;19(1):247.
88. Shah N, Deol G, McMullen E, Maazi M, Vender RB. From treatment to trigger: A systematic review of imiquimod-induced psoriasis. Int J Dermatol. 2024 May 28.
89. Gangwar RS, Gudjonsson JE, Ward NL. Mouse models of psoriasis: A comprehensive review. J Invest Dermatol. 2022 Mar;142(3 Pt B):884-897.
90. Uchino T, Kamiya D, Yagi H, Fujino-Shimaya H, Hatta I, Fujimori S, et al. Comparative analysis of intercellular lipid organization and composition between psoriatic and healthy stratum corneum. ChemPhys Lipids. 2023 Aug;254:105305.

91. Łuczaj W, Wroński A, Domingues P, Domingues MR, Skrzydlewska E. Lipidomic analysis reveals specific differences between fibroblast and keratinocyte ceramide profile of patients with psoriasis vulgaris. Molecules. 2020 Jan 31;25(3):630.
92. Školová B, Kováčik A, Tesař O, Opálka L, Vávrová K. Phytosphingosine, sphingosine and dihydrosphingosine ceramides in model skin lipid membranes: Permeability and biophysics. BiochimBiophysActaBiomembr. 2017 May;1859(5):824-834.
93. Skolová B, Janůšová B, Zbytovská J, Gooris G, Bouwstra J, Slepička P, et al. Ceramides in the skin lipid membranes: Length matters. Langmuir. 2013 Dec 17;29(50):15624-33.
94. Jennemann R, Rabionet M, Gorgas K, Epstein S, Dalpke A, Rothermel U, et al. Loss of ceramide synthase 3 causes lethal skin barrier disruption. Hum Mol Genet. 2012;21:586-608.
95. Utsunomiya A, Chino T, Utsunomiya N, Luong VH, Tokuriki A, Naganuma T, et al. Homeostatic function of dermokine in the skin barrier and inflammation. J Invest Dermatol. 2020 Apr;140(4):838-849.e9.
96. Opálka L, Kováčik A, Pullmannová P, Maixner J, Vávrová K. Effects of omega-O-acylceramide structures and concentrations in healthy and diseased skin barrier lipid membrane models. J Lipid Res. 2020 Feb;61(2):219-228.
97. Pichery M, Huchenq A, Sandhoff R, Severino-Freire M, Zaafouri S, Opálka L, et al. PNPLA1 defects in patients with autosomal recessive congenital ichthyosis and KO mice sustain PNPLA1 irreplaceable function in epidermal omega-O-acylceramide synthesis and skin permeability barrier. Hum Mol Genet. 2017;26(10):1787-1800.
98. Yokose U, Ishikawa J, Morokuma Y, Naoe A, Inoue Y, Yasuda Y, et al. The ceramide [NP]/[NS] ratio in the stratum corneum is a potential marker for skin properties and epidermal differentiation. BMC Dermatol. 2020 Aug 31;20(1):6.